MODELING FICKIAN DIFFUSION IN ASPHALT CONCRETE PAVEMENT

A Thesis

by

JULIANA EMMA CAMMARATA

Submitted to the Office of Graduate and Professional Studies of
Texas A&M University
in partial fulfillment of the requirements for the degree of

MASTER OF SCIENCE

Chair of Committee,	Anthony Cahill
Co-Chair of Committee,	Dallas Little
Committee Members,	Bruce Herbert
	David Allen
Head of Department,	Robin Autenrieth

December 2015

Major Subject: Civil Engineering

ABSTRACT

The objective of this study is to determine whether exposing an asphaltic roadway to standing liquid water for a duration of twelve hours will cause sufficient moisture penetration to induce deterioration of the roadway. A mathematical model based on mass conservation was applied for the purpose of predicting the diffusivity of moisture into the roadway. The result was then used in a computer simulation to model the temporal and spatial distribution of moisture.

In order to execute the simulation, it was necessary to determine the diffusivity of moisture in asphalt concrete. To this end, an experiment was conducted to find the change in mass over time of laboratory samples of asphalt concrete exposed to water on only one face. The procedure for executing this experiment was developed and explained as a part of the research program. The experimental data were shown to be statistically valid, and the resulting diffusivity of moisture in asphalt concrete was found to be 5.976E-5 cm^2/hr.

This value was applied within a finite element code for modeling Fick's Second Law to predict the spatial and temporal distribution of moisture within a representative roadway. Three scenarios were modeled: an undamaged asphalt concrete roadway, an asphalt roadway with a partial crack through the asphalt layer, and an asphalt roadway with a crack extending entirely through the asphalt roadway and into the base layer. On the basis of the results predicted by the model, it was concluded that an asphalt roadway is likely to experience significant damage due to moisture penetration over a twelve hour period only in the case where the crack runs entirely through the asphalt concrete layer

and into the base material. This conclusion is based on the extremely small value of experimentally observed diffusivity of moisture in asphalt concrete.

ACKNOWLEDGEMENTS

I would like to thank Dr. Dallas Little for advising me through the research and thesis process. I would also like to thank Dr. Anthony Cahill for advising me through my graduate education, and Dr. Bruce Herbert for advising in the thesis process.

I also thank Dr. David Allen, who saw in me the potential to do this work and who took it upon himself to be my guide.

Additionally, I thank Professor Matthew Bertens at City College of San Francisco for his assistance with the mathematical derivations herein, and his continued comradery. I thank Lorena Garcia Cucalon – friend and colleague – for the expertise in asphalt pavement that she so willingly shared. And I thank Richard Canatella and Tony Barbosa who oversaw my experimental research and who showed such attentiveness to my safety and wellbeing while doing so.

Finally, I thank my family – my sister, Gabriella Cammarata, who helped in the design of the figures presented in this thesis, and my parents Joanne Jackal and Salvatore Cammarata. This thesis, like everything I do, is dedicated to them.

NOMENCLATURE

FAM	Fine Aggregate Matrix
HMA	Hot Mix Asphalt Pavement
PVC	Polyvinyl Chloride
TxDOT	Texas Department of Transportation

TABLE OF CONTENTS

Page

LIST OF FIGURES

Page

LIST OF TABLES

Page

CHAPTER I

INTRODUCTION

I.1 Introduction

In the United States, approximately 2.4 million miles of paved roads are surfaced with asphalt concrete pavement (NAPA 2015). Asphalt concrete pavement is composed of 'coarse' aggregates larger than 4.75 mm in diameter of non-uniform size, shape, and mineral composition, and fine aggregates equal to or smaller than 4.75 mm in diameter, bonded together with bitumen. The affordability, availability, and reusability of asphalt have earned it an important place in any transportation engineer's toolbox. However, as successful as asphalt is as a road surfacing material, it is not without its weaknesses. It is often only as strong as the base layer beneath it, and under heavy use it warps and ravels, scattering aggregate from under tires to the roadway's periphery. As asphalt roadways see heavier use, more attention is paid to the condition and deterioration of these thoroughfares, with an eye towards cost-saving solutions. Roadway maintenance can become a financial burden on states and municipalities, especially in regions with dramatic seasonal weather patterns. Texas is one such state. With one of the fastest growing economies in the United States, the state of Texas has seen a rapid increase in the demands placed on its transportation infrastructure. In 2010-2011, the General Appropriations Act included $5.9 billion for the Texas Department of Transportation (TxDOT) to maintain and preserve the state's transportation system (Legislative Budget Board, 2011). This accounted for only 34.6 percent of TxDOT's total budget, much of which went to the construction of new roads.

Much of the asphalt degradation commonly seen in American roadways is merely the result of age. Weathering due to environmental conditions plays a role in the manner and rapidity with which asphalt pavement ages. Moisture is an especially important concern as the presence of water within asphalt during repeated-load conditions has been found to have a profound effect on roadway degradation (Kringos 2008a, Kringos 2008b, Kringos 2007, Caro 2008). Asphalt is designed to be impermeable to water, but water undoubtedly penetrates asphalt concrete, albeit at very slow rates. The wetting and drying process itself, occurring due to either atmospheric humidity or rain and flooding events, affects the bonds between asphalt and aggregate and can encourage degradation (Ghauch 2015). Once the asphalt is damaged, water may penetrate into the base layer, causing it to swell and shift, further degrading the pavement. The rate at which water damage in asphalt occurs depends on the structural integrity of the asphalt, but also on the rate at which moisture penetrates the pavement.

The purpose of this research is to illustrate and clarify the means by which moisture moves through asphalt pavement during a short-term rainfall event. Fick's Second Law is used as a model for diffusion, and the material properties of the asphalt mixture are found experimentally. These tools are used in combination with a finite element code to model and visualize the temporal and spatial distribution of moisture into a typical asphalt roadway. On the basis of these findings, future research will be proposed for mitigating the effects of such diffusion and the resulting moisture exposure.

In Chapter II, Fick's Laws will be discussed and derived for the purpose of predicting the moisture distribution within the roadway. The diffusivity values required

to employ the model developed in Chapter II will be found experimentally in Chapter III, in which the experimental procedure and results will be outlined and reviewed. The model will then be applied in Chapter IV using a finite element code designed to model diffusion using Fick's Laws. These results will be visualized using Tecplot, and conclusions will be made based on the predicted results.

I.2 Literature Review

I.2.1 Introduction

The process of moisture moving into an asphalt pavement is very slow, as asphalt is relatively impermeable. It takes years, and often a series of freeze-thaw cycles before water damage becomes apparent. However, an effect sometimes noted in asphalt pavement is a rapid decay of a roadway after a rain event. Seemingly overnight an intact portion of road will break into pieces, an apparent effect of water degradation. Substantial research seems to indicate that asphalt concrete does not undergo moisture induced damage over the short duration of a twelve hour exposure from a rain event. So what, then, could cause such a dramatic change in the condition of this pavement over such a short period of time?

There are a number of ways in which water, in either liquid or vapor form, can move through asphalt. If the environment is humid, moisture can move into the asphalt as a vapor, as the drier asphalt mix attempts to reach an equilibrium with ambient humidity (Kassem 2006, Arambula 2009, Sasaki 2006). Sasaki, et al, determined that "bituminous pavement mixtures respire (breathe) significant amounts of water every day

. . . as vapor-state permeation via connected micropores despite the impermeability to liquid water" (Sasaki 2006). Liquid water can move into asphalt from water pooling on the air-exposed surface, or water moving up from the water table, moistening the base material on the underside of the asphalt layer, which will attract moisture via capillary action (Hansson 2005). The way in which an asphalt mixture will respond to these mechanisms of moisture exposure depends significantly on its composition.

Asphalt concrete is a heavily heterogeneous material comprised of a binder, fine aggregates, coarse aggregates, and air voids (Cooley 2001, Arambula 2009). Each component of the asphalt mix is susceptible to moisture damage in specific ways. Moisture in the asphalt binder can cause a loss of adhesion between the binder and the aggregate, as well as a loss of cohesion within the binder itself (Amini 2014, Hossain 2014, Cheng 2003, Kim 2004, Raab 2012, Tarefder 2012). The degradation caused at the aggregate surface by moisture that has moved through the binder will eventually pull the mixture apart, causing stripping (Kringos 2007, Kringos 2008c, Ghauch 2015). Water will also move through the air voids in a mixture, its mobility depending largely on the mixture's porosity. 'Porous' mixes have a minimum of sixteen percent air voids, which allows water to move easily through them (EPA 2014). Typical roadway mixes fall between four and seven percent air voids, though it is often difficult to control the precise percentage due to compression during application. Because of this porosity, void space percentage, orientation, and interconnectedness greatly affect moisture penetration into asphalt (Kassem 2009, Arambula 2007). For example, it was determined in a 2005 study of diffusivity in rhyolite - a porous volcanic stone - that the diffusivity values of

moisture moving perpendicular to the rhyolite's flow structure were about five to nine times smaller than those for orthogonal and parallel directions (Yokoyama 2005). If the material has a high percentage of these interconnected void structures, the possibility of significant flow velocities within the material itself comes in to play.

Measuring and modeling flow in porous media has been heavily studied, albeit not always in relation to asphalt. Often, the techniques devised for porous media pivot on the material properties of soils, which have much greater suction and chemical reactivity than asphalt. Hysteresis, for instance, plays a large part in moisture dependent soil mechanics, while it is not clear that such an effect is as prominent in asphalt, though calibration techniques to account for phenomena like hysteresis can still be applied (Bulut 2008). Suction due to capillary action is present as a small, but measurable phenomena in asphalt (Kassem 2009). This too is mixture dependent, as coarse road materials will have weak capillarity compared to natural materials, making suction less of a concern, but rapid fluid flow a greater possibility (Hansson 2005).

The likelihood that water will move through surface pores into interconnected void spaces within the pavement is mixture dependent. For fine compositions with a lower air void percentage, it is less likely that moisture will flow through interconnected pores and more likely that diffusion will play some role in the presence of moisture in the pavement. Higher flow speeds through macropores creates the greater possibility for adhesion loss. A 2014 study by Chen, et al. found that with air void content as low as about eight percent by volume, there may be interconnected channels which allow water to easily penetrate the pavement (Chen 2014). These results, in combination with the

research in the field of porous media, suggest the possibility that rapid moisture damage may be linked to liquid water infiltration due to high void percentage in an asphalt mix, especially with the addition of cyclic loading from vehicles.

I.2.2 Modeling Moisture Transport in Roadway Materials

Once it has been established that water does move into nominally impervious asphalt pavements, the next task is to ascertain its spatial and temporal distribution. Without knowing where the water is, or how much has infiltrated, a comprehensive solution to roadway degradation due to moisture damage cannot be formulated. A common tool for modeling the volume and location of moisture in roadway materials has been Fick's Second Law, which describes diffusion from the premise of mass conservation.

Fick's Second Law assumes the diffusion coefficient to be a material property constant in time and space. Due to its porosity and heterogeneity, asphalt pavement cannot be said to have a diffusion value constant in time and space, and is therefore not truly Fickian. However, Fick's Second Law is often applied to solve diffusivity problems in porous media, and in asphalt specifically. Many researchers have investigated the validity of using a Fickian model in this way, though no consensus has yet emerged. VanMilligan compared the accuracy of Fick's Second Law and the Fokker-Planck Law and found the latter more accurate when modeling non-homogenous systems (VanMilligen 2005). VanMilligen, however, was studying the transition between gelatinous and non-gelatinous media, so while his assertion that Fick's Second Law is incomplete regarding modeling diffusion through non-homogenous systems is

valid for an asphalt model, his findings that the Fokker-Planck law is more appropriate may or may not be conclusive. Apeagyei, et al, applied both Fickian and non-Fickian (a two-phase Langmuir-type model and a two-parameter time-variable model) models to asphalt mastics, and found that all three techniques produced consistent results (Apeagyei 2015). The researchers also found that moisture diffusion depends on the phase of the water and attributed the wide range of reported diffusion values in part to unquantified effects of suction, which describes capillary action within the material void spaces (Apeagyei 2015). Often, applications of Fick's Second Law to porous media are amended to fold in coefficients representing additional material properties. Lehner, for instance, accounted for spatial variations in diffusivity via the addition of a coefficient of intrinsic conductivity (called 'K') to the diffusivity value, to correct for these shortcomings (Lehner 1979). Alternatively, Weitsman determined that the diffusivity value of Fick's Second Law needed to be amended not with intrinsic conductivity, but with an expression for temperature (Weitsman 1976). Additionally, the original Fick's Second Law expression, according to Weitsman, is accurate only for very small values of time.

In a study designed to experimentally determine the diffusivity of water in FAM, Vaconcelos, et al, used a mathematical model based on Fick's Second Law that addressed the heterogeneity of asphalt without constructing a new coefficient. The researchers modeled both infiltration of moisture into the macropores – a process dependent on hydraulic suction and flow velocity – and diffusion from the filled macropores through the mastic and aggregates, which is driven by moisture gradients

within the materials with Fickian expressions (Vasconcelos 2010). These values were added according to their percent volumes of partially and totally mobile molecules of water. In this way, Vasconcelos applied Fick's Second Law without adjusting the expression to include an additional coefficient. These researchers, along with others, have demonstrated that Fick's Second Law can be applied to moisture transport in asphalt under specific conditions. Thus, the technique can be valid when applied by conscientious hands.

I.2.3 Experimental Measurement of Diffusivity

In order to apply Fick's Second Law, researchers must experimentally measure the diffusivity of the material to be modeled. Ascertaining the diffusivity of an asphalt pavement is not an easy task, and a wide range of values have been gathered for an equally wide range of asphalt mixes (Kassem 2006, Kringos 2008b, Vasconcelos 2010, Arambula 2009). One technique, used by Kringos in her development of the RoAM software, is for researchers to find the diffusivity of binders or mastics separately from the diffusivity of aggregates and combine the two values according the asphalt mix using micromechanics (Kringos 2008a, Kringos 2008c, Kringos 2008d). Techniques to directly evaluate diffusivity values for composed asphalt concrete have also emerged. Arambula, et al. found the diffusivity of a hot mixed asphalt (HMA) by timing the movement of water vapor though an asphalt disc of uniform thickness (Arambula 2009). Kassem, et al. also considered water vapor when measuring diffusivity using thermocouple psychrometers to find suction over time (Kassem 2009). However, as

Apeagyei, et al found, water vapor cannot be assumed to behave in the same way as water in the liquid phase, and so diffusivity values must also be found using liquid water (Apeagyei 2015). Accordingly, Kassem endeavored to find the diffusivity of liquid water in fine aggregate mix (FAM) using both wetting and drying protocols to measure suction, then calculated diffusivity using Mitchel's equation (Kassem 2006). These numbers varied greatly from the numbers found in Kassem's 2009 study, mentioned above. In 2006, Kassem found that the FAM tested had diffusivity values ranging from 2.31E-4 cm^2/hr to 12.89E-4 cm^2/hr (6.43E-8 to 3.58E-7 cm^2/s). In 2009, Kassem found the HMA to have diffusivities ranging from 1.05E-2 cm^2/hr to 2.04E-1 cm^2/hr (2.92E-6 to 5.67E-5 cm^2/s) (Kassem 2009). The wide disparity between these reported values is not surprising, considering the shift in material (FMA to HMA), fluid phase (vapor to liquid), and inherent variability of asphalt. It does, however, demonstrate the difficulty researchers have encountered in accurately measuring moisture diffusivity in asphalt.

The effect of moisture on pavement performance has proven a complex and worthy topic of research. While significant work has been done in the field, much is still left unresolved regarding which diffusion models are most appropriate and what measurement techniques are the most accurate to determine material properties. The current cannon of work would be improved by the addition of an experiment that sought to measure the diffusion process in the most simple and direct way possible. On a practical scale, asphalt concrete is treated as homogenous and continuous. Why not model it thusly when finding the moisture susceptibility? With a simple experiment designed to mimic initial and boundary conditions on the partial differential equation, a

material property can be found to apply Fick's Second Law to an asphalt pavement. With such an accessible technique, diffusion values could be found quickly and easily to be used modeling asphalt at a statistically homogenous scale, allowing researchers to continue assessing the mechanisms of roadway deterioration at the practical scale.

CHAPTER II

THE MOISTURE DISTRIBUTION MODEL

II.1 Modeling Diffusion

The first set of fundamental laws describing the process of diffusion were proposed by Adolf Eugen Fick in 1855. Adolf Eugen Fick started his education in 1847 in the pursuit of mathematics and physics before deciding instead to study medicine. After studying in both Marburg and Berlin, Germany, he received his doctorate from the University of Marburg in 1851 with a dissertation on the effects of astigmatism. In 1855 his studies of the eye and its membranes led to the development of his laws of diffusion. These laws describe the diffusion of gas across a membrane, and were later found to be applicable to most fluids. He was able to double publish his law under both physiology and physics. From 1855 until his retirement in 1899 he worked as a professor of physiology at the University of Zurich, and later the Physiological Institute at the University of Würzburg. He died in 1901 ("Fick, Adolf Eugen", 2008).

Fick's Second Law is a well-known and often applied equation based on the principle of conservation of mass. It can be applied in any context in which one species is moving through another. Its applications include mechanics (force moving through a beam), thermodynamics (heat moving through an object, often called the 'heat equation'), and diffusion (fluid moving through a volume).

Fick's Second Law can be derived from the Law of Conservation of Mass. The Law of Conservation of Mass states that the mass of a closed system must remain constant over time. Therefore, the rate at which mass is added to a closed system is

balanced by the rate of change of mass within the system. To derive a conservation of mass equation, imagine a cubic control volume of a homogeneous material:

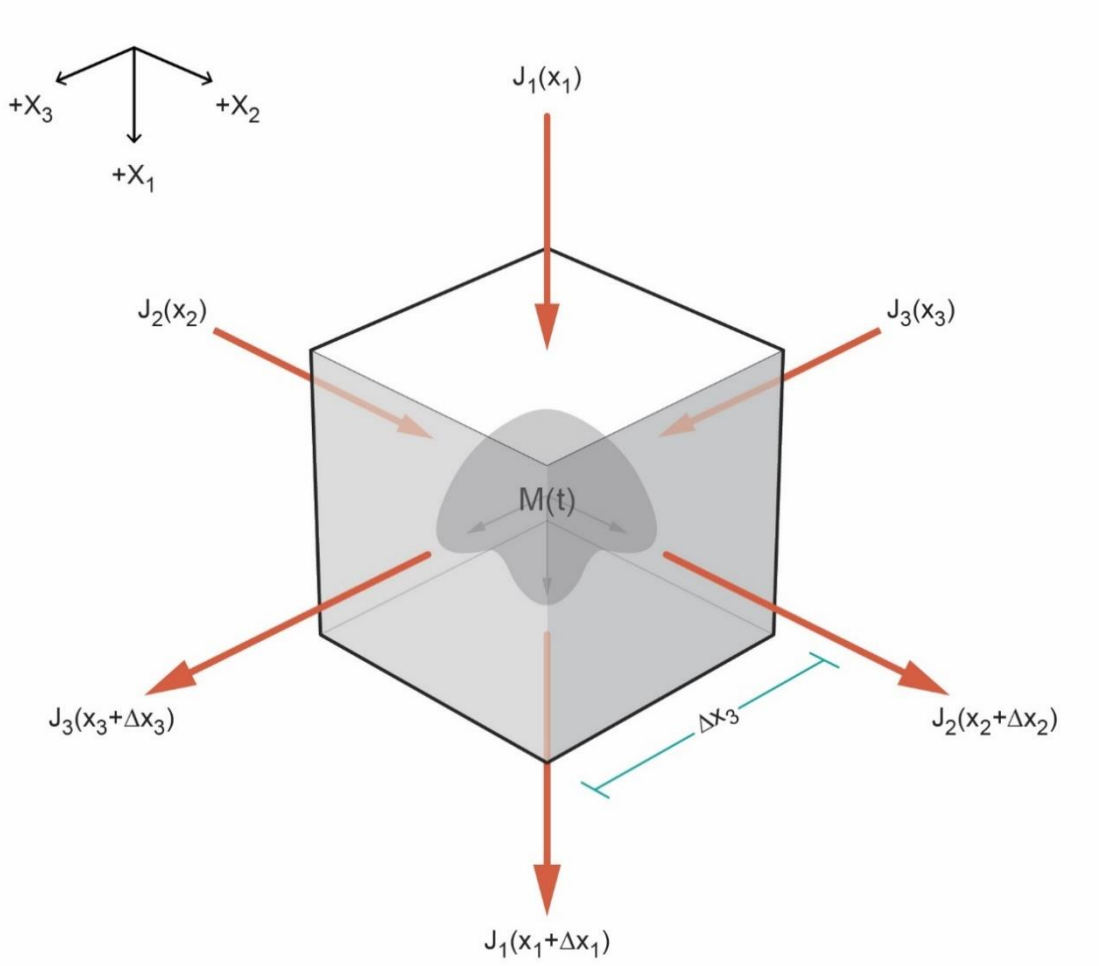

Figure 1: Three dimensional control volume, with flux

The mass flux in to the control volume must, by definition, be the difference between the mass flow *in* and the mass flow *out*. In Figure 1, flux of fluid into the control volume per unit area in the x_1 direction can be expressed as:

(1) $$[J_1(x_1) - J_1(x_1 + \Delta x_1)]\Delta x_2 \Delta x_3$$

where the $J_1(x_1)$ expression indicates flux per unit area into the control volume in the positive $x_1$direction, $J_1(x_1 + \Delta x_1)$ indicates flux per unit area out of the control volume in the positive x_1 direction, and $\Delta x_2 \Delta x_3$ is the surface area normal to the flux per unit area. The total flux can be expanded to three dimensions as follows:

(2)

$$[J_1(x_1) - J_1(x_1 + \Delta x_1)]\Delta x_2 \Delta x_3 + [J_2(x_2) - J_2(x_2 + \Delta x_2)]\Delta x_1 \Delta x_3 + [J_3(x_3) - J_3(x_3 + \Delta x_3)]\Delta x_1 \Delta x_2$$

According to the Law of Conservation of Mass, the flux of the fluid through the control volume expressed in equation (2), will equal the change in mass within the control volume over a finite period of time. The change in moisture (*M*) over a period of time (Δt starting from *t*) can be expressed as

(3) $$\frac{M(t+\Delta t) - M(t)}{\Delta t}$$

where $M(t+\Delta t)$ is the moisture density at the final time, and $M(t)$ is the moisture density at the initial time.

The total change in mass in the increment of time within the three dimensional control volume can be expressed as

(4) $$\left[\frac{m(t+\Delta t)-m(t)}{\Delta t}\right]\Delta x_1 \Delta x_2 \Delta x_3$$

where *m(t)* is the mass per unit volume.

Therefore, the complete expression of the law of conservation of mass is

(5)

$$[J_1(x_1) - J_1(x_1+\Delta x_1)]\Delta x_2 \Delta x_3 + [J_2(x_2) - J_2(x_2+\Delta x_2)]\Delta x_1 \Delta x_3 + [J_3(x_3) - J_3(x_3+\Delta x_3)]\Delta x_1 \Delta x_2 = \left[\frac{m(t+\Delta t) - m(t)}{\Delta t}\right]\Delta x_1 \Delta x_2 \Delta x_3$$

Taking limits of this equation in time and space and dividing through by the volume results in the following:

(6)

$$\lim_{x_1 \to 0}[J_1(x_1) - J_1(x_1+\Delta x_1)]\Delta x_2 \Delta x_3 + \lim_{x_2 \to 0}[J_2(x_2) - J_2(x_2+\Delta x_2)]\Delta x_1 \Delta x_3 + \lim_{x_3 \to 0}[J_3(x_3) - J_3(x_3+\Delta x_3)]\Delta x_1 \Delta x_2$$

$$= \lim_{t \to 0} \left[\frac{m(t + \Delta t) - m(t)}{\Delta t} \right] \Delta x_1 \Delta x_2 \Delta x_3$$

$$= - \lim_{\Delta x_1 \to 0} \left[\frac{J_1(x_1 + \Delta x_1) - J_1 x_1}{\Delta x_1} \right] - \lim_{\Delta x_2 \to 0} \left[\frac{J_2(x_2 + \Delta x_2) - J_2 x_2}{\Delta x_2} \right]$$

$$- \lim_{\Delta x_3 \to 0} \left[\frac{J_3(x_3 + \Delta x_3) - J_3 x_3}{\Delta x_3} \right] = \lim_{\Delta t \to 0} \left[\frac{m(t + \Delta t) - m(t)}{\Delta t} \right]$$

thereby resulting in the following partial differential equation:

(7) $$- \frac{\partial J_1}{\partial x_1} - \frac{\partial J_2}{\partial x_2} - \frac{\partial J_3}{\partial x_3} = \frac{\partial m}{\partial t}$$

If flux is confined to one dimension, in this case x_1, the Law of Conservation of Mass simplifies to the following:

(8) $$- \frac{\partial J_1}{\partial x_1} = \frac{\partial m}{\partial t}$$

According to Fick's First Law,

(9) $$J_{x_i} = -D\gamma$$

(10) $$\gamma \stackrel{\text{def}}{=} \frac{\partial m}{\partial x_i}$$

where *D* is diffusion coefficient, or diffusivity.

This law explicitly states that the amount of the species that will move through an object in a given time interval (J) is equivalent to the spatial derivative of the concentration of the species (m) in the given direction (x_i), multiplied by the diffusivity, which is a relationship between the species and the medium through which it moves. The negative sign indicates direction.

Therefore, substituting equation (9) into equation (7) results in the following,

$$-\frac{\partial J}{\partial x_i} = -\frac{\partial(-D\gamma)}{\partial x_i} = \frac{\partial m}{\partial t}$$

$$= \frac{\partial}{\partial x_i}\left(D\frac{\partial m}{\partial x_i}\right) = \frac{\partial m}{\partial t} \quad (11)$$

This is Fick's Second Law.

In the case where D is spatially constant, equation (11) simplifies to:

$$D\frac{d^2 m}{dx_i{}^2} = \frac{\partial m}{\partial t} \quad (12)$$

This equation describes a relationship in which the flow of moisture is proportional to the gradient of the moisture in the medium. In this model, D is a constant material property based on the relationship between the two media in the diffusion process. A process is 'Fickian' when diffusivity is a constant described by Fick's Second Law. Fickian materials can be accurately modeled as homogenous and continuous. Asphalt is

not Fickian, however it is common practice to model its components, especially the mastic, as such (Kringos 2007, Kringos 2008b, Aramubla 2009).

The question then becomes, under what conditions or assumptions can an asphalt mixture be modeled as spatially homogenous using Fick's Second Law? Presumably, this would be at the point of statistical homogeneity, which occurs at the smallest specimen size for which the macroscopic properties do not vary with increasing specimen size (Helms 1999). In asphalt with maximum aggregate size of 12.5 mm (0.5 in), statistical homogeneity occurs approximately at the dimension of 152 mm (6 in) cylindrical specimens of 102 mm (4 in) depth. This is the scale at which most practical concerns occur. A rain event, for instance, during which time the surface of the asphalt remains wet for several hours, would occur at the length scale at which asphalt may be considered to be statistically homogenous. It is therefore promising to investigate the possibility of accurately modeling the diffusion of moisture through asphalt using Fick's Second Law.

II.2 Numerical Model for the Experimental Determination of Diffusivity

To apply Fick's Second Law, it is necessary to experimentally determine the diffusivity of the materials under consideration. Some researchers have predicted the diffusivity of the asphalt by measuring the diffusivity of water in the components of an asphalt concrete independently from each other, then combining the materials within a micromechanics model according to the specifics of the mix (Kringos 2007, Kringos 2008a, Aramubla 2009, Cheng 2003, Kassem 2006). If the material is statistically

homogenous, then it is also possible to obtain the diffusivity directly from experiments performed on the mixture without recourse to a micromechanics model.

To determine the diffusivity of a given mix using Fick's Second Law, Fick's Second Law must first be solved for diffusivity. Partial differential equations, like Fick's Second Law, are complex and often cannot be solved in closed form. Finite element codes, like the one used later in this paper, can be utilized to obtain approximate solutions to partial differential equations with relative ease, but are designed with the assumption that the material properties are known a priori. When a material property is not known, finite element codes cannot easily be manipulated to solve for it from experimentally collected data. Fortunately, there exists an analytic solution for Fick's Second Law that can be easily replicated in the laboratory, so that for this circumstance the analytic solution can be inverted to obtain the diffusivity of the material utilized in the laboratory experiment. To demonstrate how this is applied, consider the scenario shown in Figure 2.

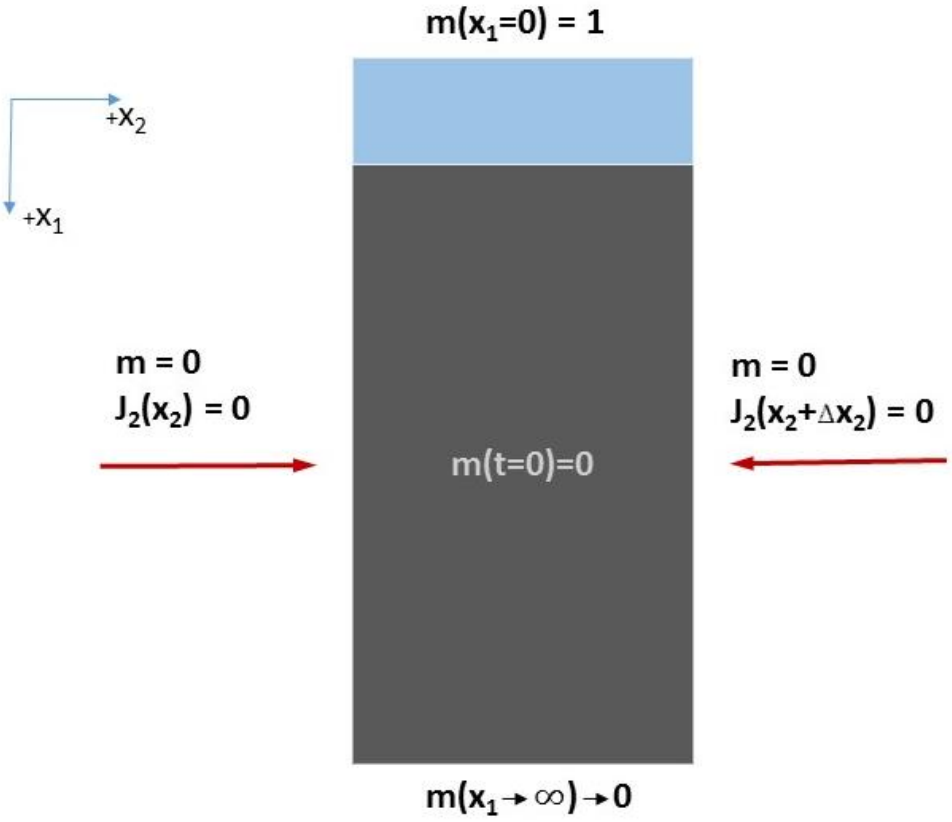

Figure 2: An object subjected to conditions producing one-dimensional diffusion in the x_1 coordinate direction.

For the conditions described in Figure 2, Fick's Second Law simplifies to the following form:

(13) $$D\frac{d^2m}{dx_1^2} = \frac{\partial m}{\partial t}$$

The initial condition defines the moisture conditions at the initial time. The sample begins with no moisture inside the asphalt, therefore the initial condition is

(14) $$m(x_1, t = 0) = 0 \qquad 0 \leq x_1 \leq \infty$$

There flux occurs only in the $x_1$direction. The sample is exposed to water on only one surface, the plane where $x_1 = 0$. On the opposing surface of the sample ($x_1 = \infty$), there is no moisture. The boundary conditions are therefore:

(15) $$m(x_1 = 0, t) = m_o \qquad 0 \leq t \leq \infty$$

(16) $$m(x_1 \rightarrow \infty, t) \rightarrow 0 \qquad 0 \leq t \leq \infty$$

It is assumed that the surface in the plane $x_1 = 0$ is in direct contact with water, therefore m_o can be set to unity.

To solve, use combination of variables by first assuming that

(17) $$m(x_1, t) = m_o \phi(\gamma)$$

(18) $$\gamma = \frac{x_1}{\delta(t)}$$

where $\delta(t)$ is an unknown function of time to be determined below.

That is, moisture at any given time and place will be initial moisture multiplied by some function of space and time. Here, γ represents a combination of the original variables in such a way that $m(x_1, t) = m_o \phi(\gamma)$ is a true statement.

To find the derivative with respect to time, use the chain rule:

$$\frac{\partial m}{\partial t} = \frac{\partial (m_o \phi(\gamma))}{\partial t} = m_o \frac{\partial \gamma}{\partial t}\left[\frac{d\left(\phi(\gamma)\right)}{d\gamma}\right] = m_o \frac{\partial \left(\frac{x_1}{\delta(t)}\right)}{\partial t}\left[\frac{d\phi}{d\gamma}\right]$$

$$= m_o \frac{d\phi}{d\gamma}\left(\frac{\partial}{\partial t}\left(\frac{x_1}{\delta(t)}\right)\right)$$

$$= -m_o \frac{d\phi}{d\gamma} x_1 \left(\frac{1}{\delta^2}\frac{d\delta}{dt}\right) = -m_o \frac{d\delta}{dt}\frac{d\phi}{d\gamma}\left(\frac{x_1}{\delta}\right)\left(\frac{1}{\delta}\right)$$

(19) $$\frac{\partial m}{\partial t} = -m_o \frac{\gamma}{\delta(t)}\frac{d\delta(t)}{dt}\frac{d\phi}{d\gamma}$$

Then take the derivative with respect to x_1:

$$\frac{\partial m}{\partial x_1} = m_o \frac{\partial \left(\frac{x_1}{\delta(t)}\right)}{\partial x_1}\frac{d\left(\phi(\gamma)\right)}{d\gamma} = m_o \frac{\partial}{\partial x_1}\left(\frac{x_1}{\delta(t)}\right)\frac{d\phi}{d\gamma}$$

(20) $$\frac{\partial m}{\partial x_1} = \frac{m_o}{\delta(t)}\frac{d\phi}{d\gamma}$$

Substituting ((20) in to the left side of (13) results in the following:

$$D\frac{\partial^2 m}{\partial {x_1}^2} = D\left[\frac{\partial}{\partial x_1}\left(\frac{\partial m}{\partial x_1}\right)\right] = D\left[\frac{\partial}{\partial x_1}\left(\frac{m_o}{\delta(t)}\frac{d\phi}{d\gamma}\right)\right] = D\frac{m_o}{\delta(t)}\left[\frac{\partial}{\partial x_1}\left(\frac{d\phi}{d\gamma}\right)\right]$$

$$= D\frac{m_o}{\delta(t)}\left[\frac{\partial \gamma}{\partial x_1}\left[\frac{d}{d\gamma}\left(\frac{d\phi}{d\gamma}\right)\right]\right] = D\frac{m_o}{\delta(t)}\left[\frac{\partial}{\partial x_1}\left(\frac{x_1}{\delta(t)}\right)\left[\frac{d}{d\gamma}\left(\frac{d\phi}{d\gamma}\right)\right]\right]$$

(21) $$D\frac{\partial^2 m}{\partial {x_1}^2} = D\frac{m_o}{\delta(t)^2}\frac{d^2\phi}{d\gamma^2}$$

Substituting equations (19) and (21) into equation (13) results in the following:

(22) $$D\frac{m_o}{\delta^2(t)}\frac{d^2\phi}{d\gamma^2}+m_o\frac{\gamma}{\delta(t)}\frac{d\delta(t)}{dt}\frac{d\phi}{d\gamma}=0$$

Multiplying both sides of equation (22) by $\frac{\delta^2(t)}{m_oD}$, the equation becomes

(23) $$\frac{d^2\phi}{d\gamma^2}+\frac{\delta(t)\gamma}{D}\frac{d\delta}{dt}\frac{d\phi}{d\gamma}=0$$

It is now time to define $\delta(t)$. In equation (17), ϕ is defined only as a function of γ. As the equation (23) now reads, ϕ will resolve to also have a time dependence. This can be addressed with the definition of $\delta(t)$ such that,

(24) $$\delta(t)\frac{\delta(t)}{dt}=constant*D$$

From equation (23),

(25) $$\frac{\delta(t)\gamma}{D}\frac{d\delta(t)}{dt}=\delta(t)\gamma\frac{constant*D}{D}=\delta(t)\gamma*constant$$

Because this can be any constant, the value 2 has been selected. The simplified expression from equation (23) is therefore

(26) $$\frac{d^2\phi}{d\gamma^2} + 2\gamma\frac{d\phi}{d\gamma} = 0$$

It is next necessary to transform the boundary conditions.

If

(27) $$m(x_1 = 0) = m_o,$$

then

(28) $$\phi(0) = 1$$

because ϕ is a function of γ, which is a function of $x_1$and time. Because the moisture at each boundary is constant at all times, at the top of the sample ($x_1 = 0$)

(29) $$\phi(0, t) = 1$$

(30) $$m(x_1 \rightarrow \infty) \rightarrow 0, \phi(\infty, t) = 0$$

If at the initial time (t=0), moisture everywhere in the sample is zero ($m(t = 0) = 0$), then the transformed initial condition is

(31) $$\phi(\gamma) = \phi\left(\frac{x_1}{\delta(0)}\right) = 0$$

For the arbitrary function $\delta(t)$, assume the initial condition is $\delta(0) = 0$. This completes the combination of variables, and equation (23) can now be solved as a set of two linear and homogeneous ordinary differential equations as expressed in equation (26) with the following initial conditions:

(32) $$\phi(o) = 1;\ \phi(\infty) = 0;\ \phi\left(\frac{x_1}{\delta(0)}\right) = 0;\ \delta(0) = 0$$

The general solution for equation (26) is given by:

(33) $$\phi(\gamma) = a_1 + a_2 \int_0^{\gamma} e^{-\beta^2}\, d\beta$$

When the boundary conditions described in equation (32) are applied to equation (33), the result is

(34) $$\phi(\gamma) = 1 - \text{erf}(\gamma) = erfc(\gamma)$$

With the initial conditions described in (32), in combination with equation (24), γ can also be defined. Substituting the results into equation (18), the expression for γ becomes:

(35) $$\gamma = \frac{x_1}{\delta(t)} = \frac{x_1}{2\sqrt{Dt}}$$

Finally, substitute equation (34) into the expression for $m(x_1, t)$ (equation (17) to obtain the following:

(36) $$m(x_1, t) = m_o \phi(\gamma) = m_o \, erfc(\gamma)$$

Therefore,

(37) $$m(x_1, t) = m_o \, erfc\left(\frac{x_1}{2\sqrt{Dt}}\right)$$

The above equation satisfies the initial and boundary conditions (see Appendix B) and can be shown to be the solution to the scenario described by Figure 2 by direct substitution in to the governing equation as done in the proof of the derivation for *D* in Appendix C. With this result, it is possible to invert this expression to produce an equation for diffusivity in terms of experimentally observed quantities.

Equation (37) describes the moisture distribution in the medium at a given time. If this expression is integrated over the volume of the sample, the result is the total moisture, *M(t)*, in the three dimensional medium at a given time:

(38) $$M(t) = \int m(x_1, t) \, dV = \int m(x_1, t) \, dx_1 dx_2 dx_3$$

For the case in which the experimental specimen is symmetric and uniform in the x_2 and x_3 coordinates, equation (38) simplifies to:

(39) $$M(t) = A\int_0^\infty m(x_1, t)dx_1$$

where A is the cross-sectional area of the specimen.

The total change in mass due to water diffusing into the material over a defined length of time can be measured experimentally. It is therefore possible to determine *D* from this experiment.

To do this, first substitute equation (37) into equation (39) and integrate the result to obtain the following equation for the total mass at any given time:

(40) $$M(t) = Am_o\int_0^\infty erfc\left(\frac{x_1}{2\sqrt{Dt}}\right)dx_1$$

In order to simplify the above equation, the following change of variables is introduced:

(41a) $$z = \frac{x_1}{2\sqrt{Dt}}, \qquad dz = \frac{1}{2\sqrt{Dt}}dx_1,$$

and

(41b) $$dx_1 = dz(2\sqrt{Dt})$$

Substituting equations (41a) and (41b) into equation (40) therefore results in the following equation for the total change in mass, *M(t)*, as a function of time:

(42) $$M(t) = Am_o(2\sqrt{Dt})\int_0^\infty \mathrm{erf}\,c(z)dz$$

To simplify, divide both sides by the constant expression $Am_o(2\sqrt{Dt})$:

(43) $$\frac{M(t)}{Am_o(2\sqrt{Dt})} = \int_0^\infty \operatorname{erf} c(z)dz$$

The integration of equation (43) can be found in Appendix A. The result when $m_o = 1$ is

(44) $$D = \frac{M(t)^2\pi}{4A^2t}$$

To prove that this result is valid, substitute (37) and (44) into (13). This proof can be found in Appendix C.

It has now been established that diffusivity can be expressed as a function of material properties which are either easily measurable or controlled. At this point an experiment can be designed to find the mass of moisture in the sample after a defined time interval under the same initial and boundary conditions as generates the error function solution.

CHAPTER III

EXPERIMENTAL DETERMINATION OF ASPHALT CONCRETE DIFFUSIVITY

As discussed in Chapter II, to apply the equation for diffusivity derived from the error function solution to Fick's Second Law, an experimental protocol must be designed that matches the initial and boundary conditions that produce the analytic result obtained in equation (44). Accordingly, an experiment has been devised that is in agreement with the scenario posed in Chapter II. A schematic of this experiment is presented in Figure 3.

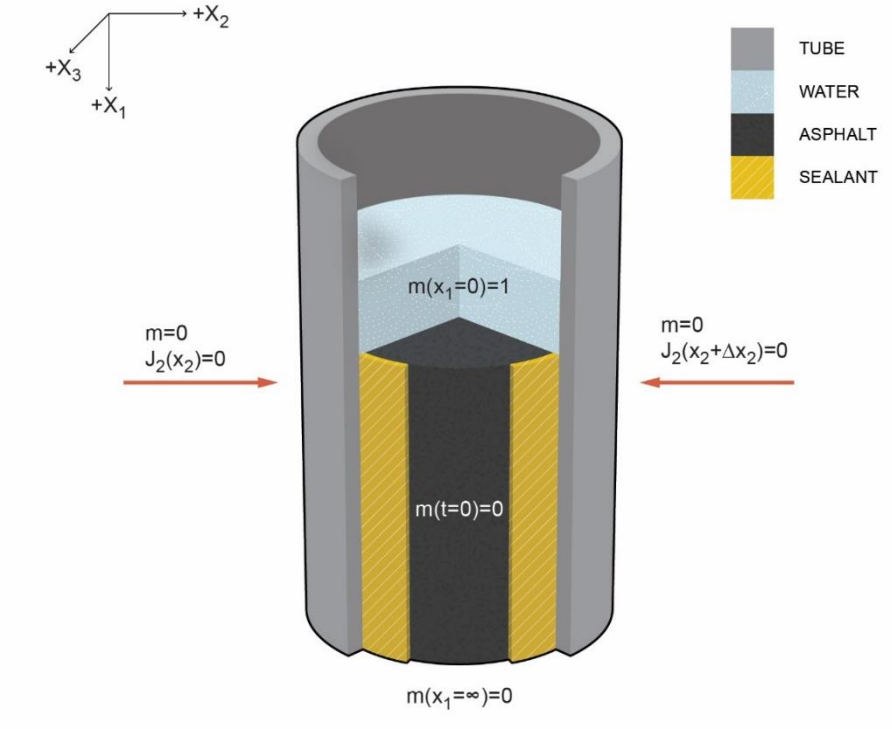

Figure 3: Experimental assembly for determining the diffusivity of moisture in asphalt concrete

As shown in Figure 3, a cylindrical specimen of asphalt concrete is sealed into a polyvinyl chloride (PVC) tube, allowing water to be exposed only to the top surface of the specimen. This geometric configuration allows water to diffuse only in the positive x_1 direction, without subjecting the sample to pressure from the top or sides, which might adversely affect the experimental results. Once the asphalt concrete, tube, and sealant are assembled, the mass of the specimen is measured. Water is then poured onto the top surface of the specimen, thereby matching the saturation boundary condition described in Chapter II. The total mass of the specimen is then measured at predetermined intervals, and the initial mass is subtracted from this value to obtain the mass of water that has diffused into the asphalt sample during the elapsed time. This is the *M(t)* value needed to solve for the diffusivity in equation (44). The other values – $m_o, A,$ and t – are known and controlled by the experimenter.

Because the phenomenon under consideration is water diffusion in asphalt during a rain event, it was decided that an experiment would be run for a total time span of twelve hours. Diffusion values after that amount of time would not be representative of diffusion during and immediately after a rain event. For the samples to be weighed, the water would have to be poured off of them, which could potentially disrupt the aggregate at the surface and corrupt the absorption values. For this reason, mass values were measured every two hours. This limited the number of times the sample was disturbed, while allowing for large enough time intervals at high enough frequency to observe a change in absorption in time.

III.1 Experimental Setup

The asphalt tested is a fine surface mixture, TxDOT classification Type D limestone, PG 64-22. This mix has a conventional binder with no polymer modifications, and a maximum aggregate size of 12.5 mm. Because this test is designed to measure changes on a large length scale, a banal asphalt mix was assumed to be most representative. Type D PG 64-22 is a typical wearing surface in Texas and was taken from a working road crew. The theoretical maximum specific gravity, or "Rice" gravity, was calculated to be 2.453. This value is the ratio of the mass of a unit volume of non-compacted asphalt mixture to the mass of an equal volume of water and represents the specific gravity of the asphalt excluding air voids. The plant mixed asphalt mixture was heated to 135° C and compacted by a Superpave gyratory compactor into 152.4 mm diameter by 70 mm specimens.

Figure 4: Asphalt cores

As shown in Figure 4, each specimen was then cored into four 51 mm diameter cores, and labeled according to source specimen and order of coring (i.e. a core labeled 2-4-14-1 would be the first core taken from specimen 2-4-14). The density and void space percentage of each core was found using a saturated-surface-dry technique. Mass and void percentage values for each sample used in the final test can be found in Appendix D. Void percentages ranged from 6.69% to 10.23%, with the majority of the samples being in the 9.22% to 9.85% range. Probably due to the small number samples used, void percentage did not show a strong correlation with moisture uptake values found during the experimental process. The dimensions of the specimens (70 mm by 51 mm diameter) were chosen to accommodate the measurement range of the scale

available for mass measurements. The Sartorius scale used (see Figure 5) measures up to 620 g with a sensitivity in the third decimal.

Figure 5: Sartorius 620g scale

Because the predicted mass changes are quite small, it is crucial to utilize a scale with at least this level of sensitivity. However, scales can rarely measure both the large masses of asphalt samples and fluctuations in the third decimal. Therefore, the samples needed to be cored as small as possible to limit mass. With an asphalt mix containing a maximum aggregate diameter of 12.5 mm, specimens smaller than 51 mm in diameter would likely introduce large statistical variations in measured diffusivity. Additionally, to approximate an infinite specimen depth, the samples should be several times longer

than the deepest predicted point of water infiltration. After observing moisture diffusion in preliminary tests for each expected void percentage, seventy millimeters was selected as the shortest viable specimen depth. The final dimensions of the asphalt specimens were 70 mm with a 51 mm diameter. Based on the findings of Helms, et al, these dimensions should be sufficient to produce accurate values for a model that assumes statistical homogeneity of the media (Helms 1999).

PVC was selected for the tube. JM Eagle 51 mm by 3 m (2 in by 10 ft) Schedule 40 conduit was selected. This piping has a four millimeter wall thickness. Three 3 m pipes were cut in to twenty-eight, 108 mm long pieces. Some of these pieces were discarded, the rest were cleared of sawing debris and weighed before assembly (see Figure 6).

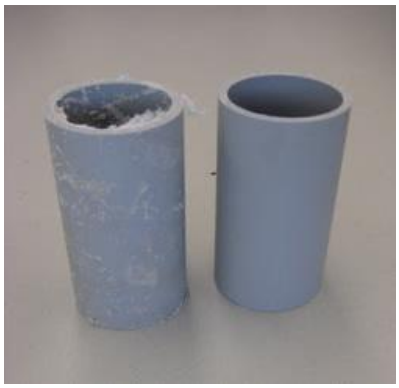

Figure 6: PVC preparation

An absorption test was run on the PVC material and it was found that, in terms of area directly exposed to water, the piping absorbs 1.09E-4 grams of water per inch squared per hour. Since only 1.68 in^2 of PVC surface area in each assembly was exposed to water, only $6.27x10^{-5}$ grams of water were taken up by the PVC each hour. The asphalt test was run for twelve hours, at which point the predicted mass of water absorbed by the PVC would be $7.52x10^{-4}$ g. The process by which these numbers were attained is explained fully below. Because this amount would not register on the 620g scale, it does not contribute significantly to the experimentally measured change in mass of the specimen and was therefore not taken in to account in the mass calculations.

One of the most challenging parts of the experimental setup was finding an appropriate sealant for the cylindrical sides of the specimens. The asphalt samples needed to be completely sealed in to the PVC such that no diffusion of water occurred on the lateral specimen boundaries. After careful review of a number of commercial sealants, epoxy was chosen as the most appropriate based on its low water diffusivity, low viscosity, and its behavior as a PVC lubricant. While the epoxy effectively creates a seal between the asphalt and the PVC due to both adhesive and compressive forces, when dry it can be broken free from the PVC cleanly and relatively easily, enabling better control of the location and amount of sealant. A variety of epoxies were considered, and Devcon Home 5-Minute Epoxy (DEV20945) was selected for its ease of use and low price.

A simple test was run to assess the absorptiveness of the DEV20945 and the JM Eagle 51 mm by 3 m Schedule 40 conduit. For the PVC test, a piece of 108 mm long

clean PVC was selected. One 13 mm was measured and marked from the bottom of the tube, and the tube was weighed dry. The tube was then placed in a large glass beaker into which distilled water was poured until it reached the 13 mm mark. The beaker was covered with plastic to prevent evaporation and contamination and left to sit for twenty four hours. After twenty four hours, the tube was removed from the bath, thoroughly patted dry, and weighed again. The difference in mass between the dry weight and wet weight was used to calculate absorption per hour. Exposed surface area was calculated using the interior, exterior, and thickness specifications given by JM Eagle (Table 1).

For the epoxy test, another piece of PVC, 108 mm long, was selected, cleaned and weighed dry. A 13 mm line was marked along the inside perimeter of the tube, and a 13 mm mark made on the outside of the tube. Epoxy was then spread along the inside of the tube to the 13 mm mark and left to dry for the full curing time – twenty four hours. The tube with the epoxy ring is pictured in Figure 7. Once the epoxy cured, the tube was

Figure 7: Epoxy application

again weighed. It was then placed in a beaker, and distilled water was added until it reached the 13 mm mark. The beaker was covered with plastic and let to sit for twenty four hours. The setup is pictured in Figure 8. The tube was removed from the water,

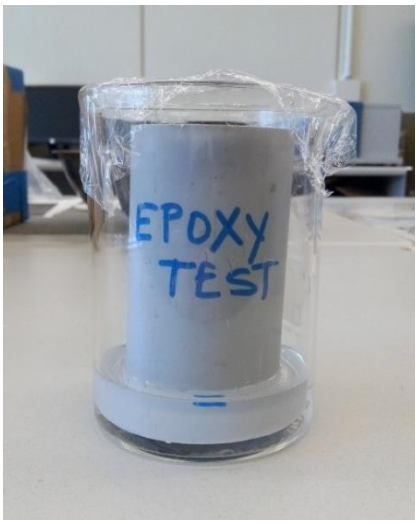

Figure 8: Partial submersion

patted dry, and weighed a final time. The exposed area of the PVC was again found using the specifications given by JM Eagle. The surface area of the PVC included the 13 mm around the outside of the tube as well as the 4 mm width of the tube. The surface area of the epoxy was calculated similarly using the inner diameter of the tube and accounting for an average 2 mm ring of settled epoxy. The addition of these small

measurements of area did not result in a measurable difference in absorption rates. The results are recorded in Table 1.

PVC		**EPOXY**	
Initial Mass [g]	118.281	**Initial Mass [g]**	119.770
Mass After 24 hrs [g]	118.293	**Mass After 24 hrs [g]**	119.938
Change in Mass [g]	0.012	**Change in Mass [g]**	0.168
Inner Diameter [in]	2.067	**Area of Epoxy [in^2]**	3.758
Outer Diameter [in]	2.375	**Area PVC [in^2]**	4.731
Thickness [in]	0.154	**Water Absorbed by PVC [g/24hr]**	7.12E-03
Area of PVC exposed [in^2]	7.978	**Water Absorbed by EPOXY[g/24hr]**	0.161
Change in Mass Per Unit Area [g/in^2*24hr]	1.50E-03	**Change in Mass Per Unit Area [g/in^2*24hr]**	0.043
Change in Mass Per Unit Area [g/in^2*hr]	6.27E-05	**Change in Mass Per Unit Area [g/in^2*hr]**	0.002
After 12 Hrs	7.52E-04	**After 12 Hrs**	0.021
		Average Area of Epoxy [in^2]	1.023
		Average Absorption [g/hr]	0.002

Table 1: Absorption tests

The quantity of epoxy needed for assembly was determined to be approximately twenty five milliliters per sample. With over forty samples assembled between practice and experimental trails, the amount of epoxy required to seal all of the specimens had the potential to be very costly. Because there was no record found of an experiment of this kind, it was unclear whether such a financial investment would be cost effective. DEV20945 is affordable and easy to apply, and the absorption test found it to take on only 0.002 g/in^2hr of water. Surface area was used in absorption calculations instead of mass because the surface area exposed to water is easily approximated. Ascertaining how much of the mass of the epoxy was in direct contact with the water would require calculations based on surface area measurements, thereby producing potential erroneous experimental measurements. After measuring the thickness of the epoxy rings in the radial coordinate direction on the samples used for testing (see Figure 3), four millimeters was found to be the average thickness of the epoxy ring exposed to water. As shown in Table 1, the mass of the water absorbed by the epoxy per sample per hour was found to be 0.002 g/hr. While suitably low, this is not an insignificant finding, considering the small masses measured in this experiment. This value was therefore taken into account when calculating final moisture values for the samples.

III.2 Specimen Assembly

Fifteen asphalt cores were chosen for experimentation based on their structural stability and uniformity of shape. The diameter of each core was measured with a caliper and its mass was weighed on the Sartorius 620g scale. Fifteen PVC tubes were selected and

labeled to match the cores. The arrangement is pictured in Figure 9. They were each then weighed and their masses recorded. Each asphalt sample was thinly but thoroughly coated with the DEV20945, as demonstrated in Figure 10. After each sample was coated, the corresponding PVC tube was lowered onto it from above (see Figure 11).

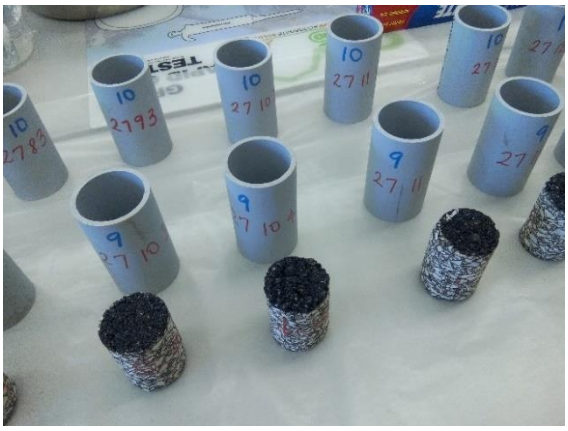

Figure 9: Asphalt cores and tubes (note: inner tube diameter is 51 mm [2 in]).

Figure 11: Application of epoxy

Figure 10: Assembly

The space between the asphalt core and the PVC tube was then filled from above using a pipet tip attached to a bag, as shown in Figure 12 and 13. This was left to sit for the duration of the initial curing time of the epoxy (one hour). Additional epoxy was

Figure 12: The piping tool used for epoxy. Pre-assembled (left) and assembled (right).

then piped on to the sample to ensure that the asphalt core was completely sealed into the PVC tube. This assemblage was left to sit for the full curing time of the epoxy (twenty-four hours). Once the epoxy had cured, each sample was again weighed. To prevent mass losses due to crumbling on the exposed bottoms of the samples, a small piece of cellophane was secured to the bottom of each specimen with a rubber band (see Figure 14). The samples were then weighed again and their final dry weights recorded.

Figure 13: The piping tool with epoxy (left) and in use (right)

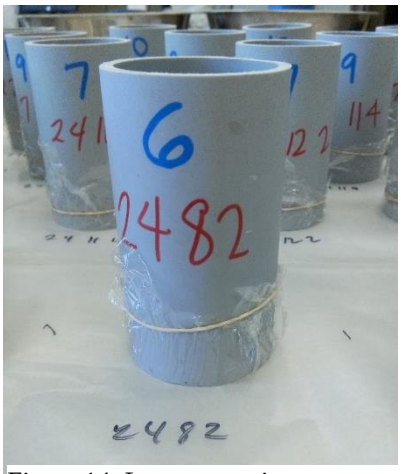

Figure 14: Loss prevention

A vertical distance of 0.5 in was measured from the top of each asphalt core and marked on the inside of the PVC tube, as shown in Figure 15. This indicated the water level

Figure 16: High water mark

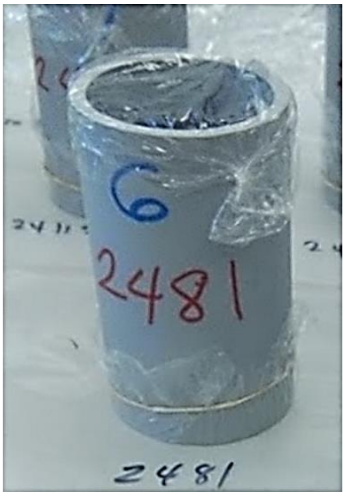

Figure 15: Sample specimen

that would be maintained on each sample at all times except during weighing.

The samples were initially arranged on a table on top of sheets of waxed paper, then later on brown paper towel so that any leaks could be quickly recognized and the samples removed. Distilled water was poured to the water lines of each sample and the samples were covered with another small piece of cellophane, both to prevent debris from falling in and to minimize the possibility of evaporation (see Figure 16).

III.3 Measurement Procedure

As described in Chapter II, the purpose of the experiment was to measure the amount of moisture that diffuses into the asphalt concrete ($M(t)$). While this would seem a straightforward process, there were a number of difficulties. One of the samples (Sample 24123) leaked immediately. This was not unexpected. In previous testing, upwards of

thirty percent of the samples leaked with the first pour. This leakage is likely due to the high porosity of asphalt and its uneven surfaces, which are difficult to seal. None of the epoxies tested produced better performance against leakage, nor did any of the many application techniques tested. Since leakage prevents the accurate measurement of moisture uptake, all specimens that leaked were removed from consideration.

Before two hours had elapsed, another sample (Sample 24121) leaked. Between two and four hours Sample 2744 leaked, and finally between four and six hours two more samples leaked (Samples 24122 and 2793). These were the last samples to leak, leaving ten viable samples. A piece of aggregate spalled off of Sample 24114 during the drying process before the second weighing, so that mass values were not recorded for that sample after two hours. The remaining samples were then weighed three more times. The experimental results are shown in Table 2.

Sample	Mass @ t=1 (2hr) [g]	Mass @ t=2 (4hr) [g]	Mass @ t=3 (6hr) [g]	Mass @ t=4 (8hr) [g]	Mass @ t=5 (10hr) [g]	Mass @ t=6 (12hr) [g]
24114	422.809	-	-	-	-	-
24121	-	-	-	-	-	-
24122	420.647	420.688	-	-	-	-
24123	-	-	-	-	-	-
24143	429.517	429.589	429.602	426.616	429.636	429.669
2711	418.772	418.861	418.951	418.894	418.925	418.763
2744	420.698	-	-	-	-	-
2793	423.620	423.522	-	-	-	-
27102	412.917	412.954	412.947	412.982	412.967	412.995
27103	417.243	417.193	417.256	417.234	417.272	417.278
27111	414.877	415.000	415.045	415.016	414.949	414.943
27113	417.593	417.935	417.963	418.035	417.809	417.910
27121	415.805	415.876	415.846	415.862	415.884	415.852
27122	416.072	416.306	416.279	416.325	416.321	416.307
27123	416.042	416.110	416.187	416.148	416.192	416.208

Table 2: Twelve hour test results

III.4 Analysis of the Experimental Results

The results of the timed absorption test were placed in an Excel file and adjusted for moisture absorption into the epoxy, as described above. The experimentally measured changes in mass were then substituted into equation (44) to calculate the diffusivity of the samples. The results are shown in Table 3 and Figure 17.

Sample	Diff. @ t=1 [cm^2/hr]	Diff. @ t=2 [cm^2/hr]	Diff. @ t=3 [cm^2/hr]	Diff. @ t=4 [cm^2/hr]	Diff. @ t=5 [cm^2/hr]	Diff. @ t=6 [cm^2/hr]
24143	7.44E-05	5.95E-05	4.19E-05	3.34E-05	2.93E-05	2.86E-05
2711	2.25E-04	1.58E-04	1.42E-04	8.68E-05	7.62E-05	3.32E-05
27102	2.33E-04	1.34E-04	8.57E-05	7.30E-05	5.42E-05	4.98E-05
27103	1.71E-04	6.36E-05	5.86E-05	3.85E-05	3.67E-05	3.10E-05
27111	1.71E-04	1.46E-04	1.13E-04	7.53E-05	4.50E-05	3.59E-05
27113	8.93E-05	2.14E-04	1.54E-04	1.41E-04	5.21E-05	6.26E-05
27121	5.48E-05	4.66E-05	2.42E-05	2.00E-05	1.83E-05	1.17E-05
27122	7.33E-05	1.35E-04	7.90E-05	7.09E-05	5.50E-05	4.25E-05
27123	8.44E-05	6.52E-05	6.49E-05	3.89E-05	3.85E-05	3.41E-05

Table 3: Diffusivity values

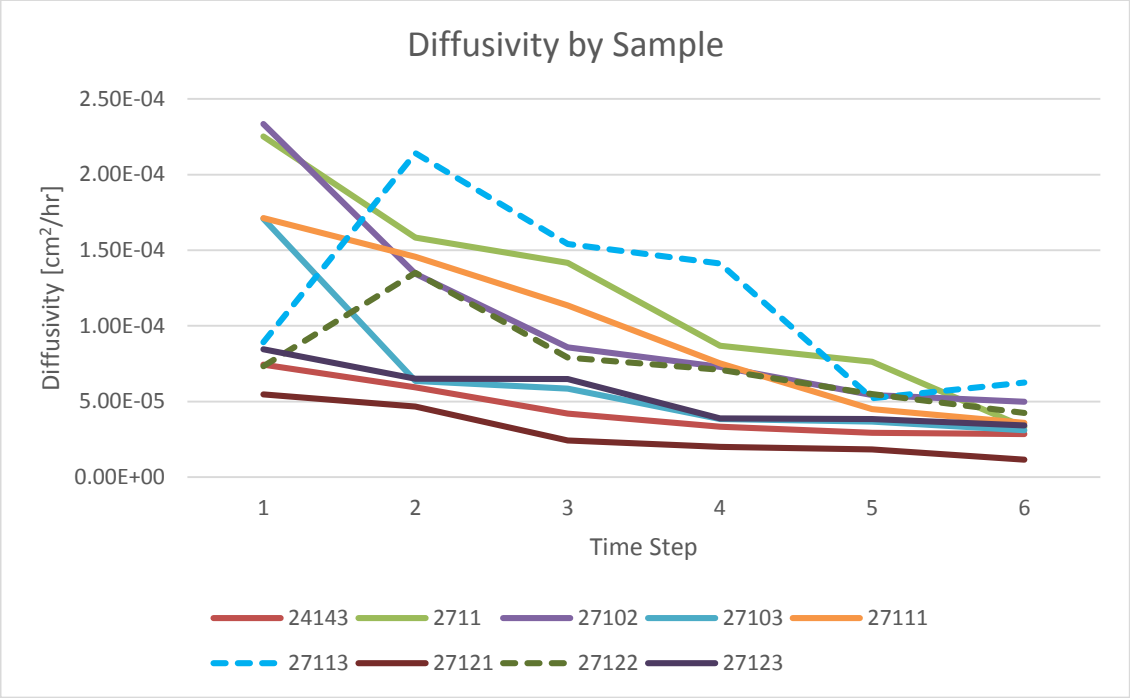

Figure 17: Diffusivity values

From Figure 17, it is clear that two of the samples - Sample 27113 and Sample 27122 - have diffusivity patterns that dramatically increase at the second time step. These readings are likely inaccurate and due to water slipping between the tube and epoxy, rather than moving through the asphalt. If they were accurate, they would represent a physical anomaly in the asphalt, like a large, interconnected void structure. In either case, the unusual pattern justifies that diffusivity measurements for these two samples be discarded.

The data were then grouped by time step and further analyzed using the JMP statistical discovery software (see Figure 18) (SAS Institute Inc., 2013). The JMP output

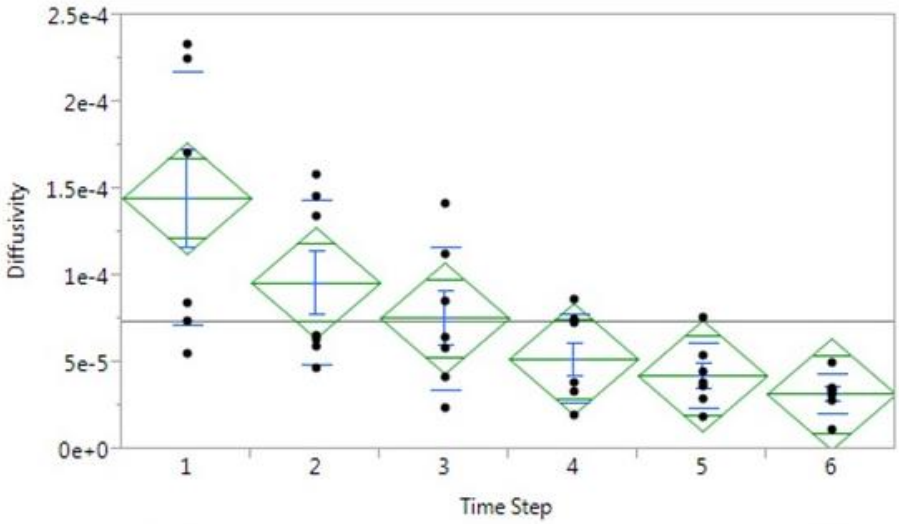

Means and Std Deviations

Level	Number	Mean	Std Dev	Std Err Mean	Lower 95%	Upper 95%
1	7	0.000145	0.000073	2.77e-5	7.7e-5	0.00021
2	7	0.000096	0.000048	1.8e-5	5.22e-5	0.00014
3	7	0.000076	0.000041	1.55e-5	3.78e-5	0.00011
4	7	0.000052	0.000026	0.00001	2.86e-5	7.59e-5
5	7	0.000043	0.000019	7.05e-6	2.53e-5	0.00006
6	7	0.000032	0.000011	4.26e-6	2.16e-5	4.25e-5

Summary of Fit

Rsquare	0.493375
Adj Rsquare	0.42301
Root Mean Square Error	4.174e-5
Mean of Response	0.000074
Observations (or Sum Wgts)	42

Connecting Letters Report

Level		Mean
1	A	0.00014480
2	B	0.00009613
3	B C	0.00007576
4	B C	0.00005227
5	C	0.00004260
6	C	0.00003204

Levels not connected by same letter are significantly different.

Means for Oneway Anova

Level	Number	Mean	Std Error	Lower 95%	Upper 95%
1	7	0.000145	1.58e-5	0.00011	0.00018
2	7	0.000096	1.58e-5	6.41e-5	0.00013
3	7	0.000076	1.58e-5	4.38e-5	0.00011
4	7	0.000052	1.58e-5	0.00002	8.43e-5
5	7	0.000043	1.58e-5	0.00001	7.46e-5
6	7	0.000032	1.58e-5	5.05e-8	6.4e-5

Std Error uses a pooled estimate of error variance

Figure 18: JMP output for all data

plot highlights the data's curved decay shape, indicative of a boundary effect. It is also clear, though, that as the diffusivity values decrease, so does the standard deviation of the data in each time step. The standard deviation at time step 1 is almost seven times the

standard deviation of time step 6. This indicates that the results are trending towards more Fickian behavior as the experiment progresses.

From an initial analysis of this data, it is clear that time step 1 is an outlier. The 'Connecting Letters Report' in Figure 18 clearly illustrates that time step 1 shows statistical similarities with none of the other time steps. The diffusivity values at time step 1 are higher, on average, than at the other time steps, and all but one of the data points can be considered statistical outliers. This is not surprising considering time step 1 marks the first exposure to moisture. It is likely that these high, unevenly distributed values are due to rapid filling of the surface layer of asphalt pores, rather than indicative of diffusion into the material. Therefore, another statistical analysis was conducted without the inclusion of the data set from time step 1. The results are pictured in Figure 19. The results when the data set is limited to time steps 2 thru 6 appear more consistent.

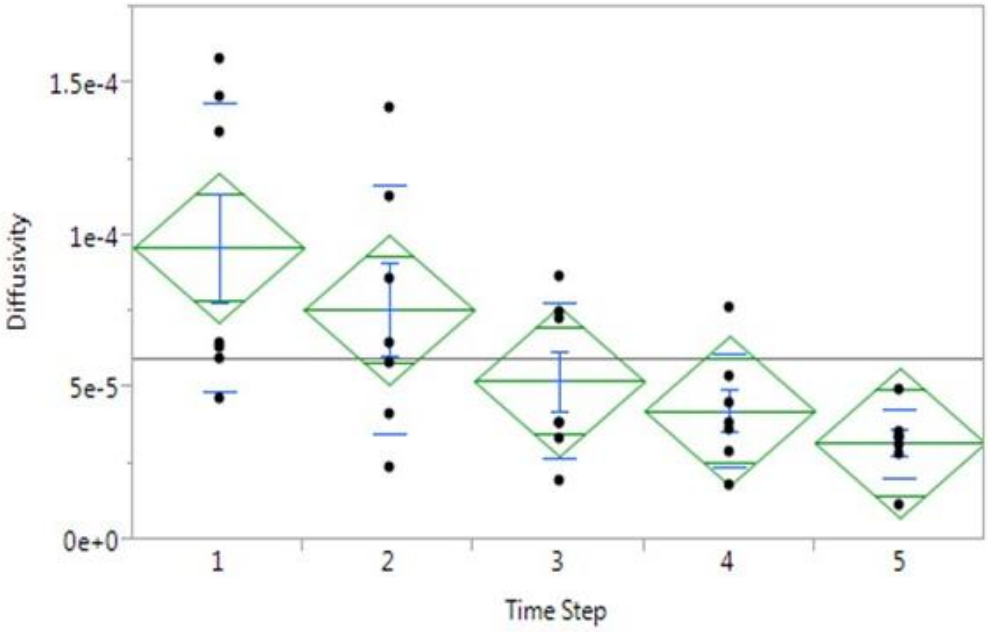

Means and Std Deviations

Level	Number	Mean	Std Dev	Std Err Mean	Lower 95%	Upper 95%
1	7	0.000096	0.000048	1.8e-5	5.22e-5	0.00014
2	7	0.000076	0.000041	1.55e-5	3.78e-5	0.00011
3	7	0.000052	0.000026	0.00001	2.86e-5	7.59e-5
4	7	0.000043	0.000019	7.05e-6	2.53e-5	0.00006
5	7	0.000032	0.000011	4.26e-6	2.16e-5	4.25e-5

Summary of Fit

Rsquare	0.382992
Adj Rsquare	0.300724
Root Mean Square Error	3.184e-5
Mean of Response	5.976e-5
Observations (or Sum Wgts)	35

Means for Oneway Anova

Level	Number	Mean	Std Error	Lower 95%	Upper 95%
1	7	0.000096	1.2e-5	7.15e-5	0.00012
2	7	0.000076	1.2e-5	5.12e-5	0.00010
3	7	0.000052	1.2e-5	2.77e-5	7.69e-5
4	7	0.000043	1.2e-5	1.8e-5	6.72e-5
5	7	0.000032	1.2e-5	7.46e-6	5.66e-5

Std Error uses a pooled estimate of error variance

Figure 19: JMP output for time steps 2 thru 6

Both the standard error values and the root mean square errors have decreased by 24% from the complete data set. The root mean square error is still, however, larger than half

of the value of the mean. The R^2 value is lower than the previous test, indicating less linearity in the data. Because Fick's Second Law assumes constant diffusivity in time, the results indicate that the response is somewhat non-Fickian. However, because of the boundary effect where high connectivity in the first half centimeter of asphalt allows water to move quickly into the surface of the pavement, non-linearity in the data must be accepted. In addition, there could be other physical and chemical reasons for non-Fickian behavior (Cai 1994). The decreased root mean square error of this data set indicates it is the more statistically consistent data set despite the irregularities. Therefore the mean value from this data set is the best representation of the diffusivity value. The mean for this set of values is 5.976E-5 cm^2/hr.

It is not common to use liquid water in tests to measure the diffusivity of asphalt concrete. It is far more common to use water vapor via a relative humidity chamber, and therefore most experimentally measured asphalt diffusivity values are for water vapor and cannot conclusively be compared to the liquid water value found here. However, this value is smaller than the diffusivity values for liquid water through FAM mix found by Kassem, et al in 2006, which ranged from 2.31E-4 cm^2/hr to 12.89E-4 cm^2/hr, depending on the mix (Kassem 2006). An additional study in 2010 using FAM and liquid water, however, found diffusivity values ranging from 4.39E-5 cm^2/hr to 8.03E-5 cm^2/hr (1.22E-12 to 2.23E-12 m^2/s) (Vasconcelos 2010). The diffusivity value found in the experiment described here is similar the values found by Vasconcelos in 2010. It should be noted that the earlier experiments tested FAM, which can be expected to have a lower diffusivity than composed asphalt, as the finer aggregate size results in fewer air voids.

This would imply that the diffusivity value found in this experiment may be low for composed asphalt pavement. However, because the detailed specifications of the mix used in this experiment are not known, it is not possible to better correlate the diffusivity value calculated with values found by other researchers with more specific mixes. It is clear, however, that this value falls within or near the range of diffusivity values found for similar materials.

CHAPTER IV

MODEL FOR PREDICTING MOISTURE DIFFUSION IN ROADWAYS

IV.1 Finite Element Code for Diffusion

When the diffusion value for water in a material is known, a finite element code can be used to model the distribution of moisture using Fick's Second Law under assigned boundary and initial conditions. Toward this end, an in-house finite element code was used to model the diffusion of moisture into roadways. The formulation for this code can be found in J.N. Reddy's *An Introduction to the Finite Element Method* (Reddy 1993). The code models the initial boundary problem outlined in Chapter II, for which the initial and boundary conditions are described in equations (14) thru (16).

IV.2 Code Verification

To verify the finite element code, several scenarios were simulated. The results were then compared to either analytic solutions or computational solutions obtained by other models. The first test case simulated one dimensional, steady state diffusion to solve the simplified Fick's Second Law equation:

(45) $$D\frac{d^2m}{dx_1^2} = \frac{\partial m}{\partial t}$$

This equation calculates change only in the x_1 direction. The closed form solution of the above equation was found to be:

(46) $$m(x) = -c_1 x - c_2$$

where c_1 and c_2 are obtained from the boundary conditions.

Using the closed form solution to verify the finite element solution, a steady state reaction through a ten element section of material, each triangular element defined by three nodes, was input into the code with boundary conditions of *M(1) = 100* and *M(4) = 0*, where 1 and 4 are nodes, not coordinates on the x-axis. For simplicity, *D* was set to equal 1, as was density. The code was found to generate accurate moisture values according to the analytic solution. The Fortran input code for this scenario can be found in Appendix F. The finite element code was then used to simulate a one-dimensional transient problem. The Crank-Nicolson method was used to find the integration constant 0.5, which worked best for the given calculations (Reddy 1993). The diffusion code was run with two elements through a transient reaction with solution steps increased from one (used for steady state) to ten. The code was then run with ten elements through a transient reaction with solution steps increased from ten to one hundred, then finally with twenty elements through a transient reaction with on hundred solution steps. The twenty element input code can be found in Appendix F.

The analytic solution for this problem is the complementary error function given by equation (37) in Chapter II. The finite element code was run with boundary conditions of *M(1) = 1* and *M(22) = 0* and the results were verified first by using a second Fortran erf code (Figure 20), then by using a Matlab erfc program, as shown in Figure 21.

.

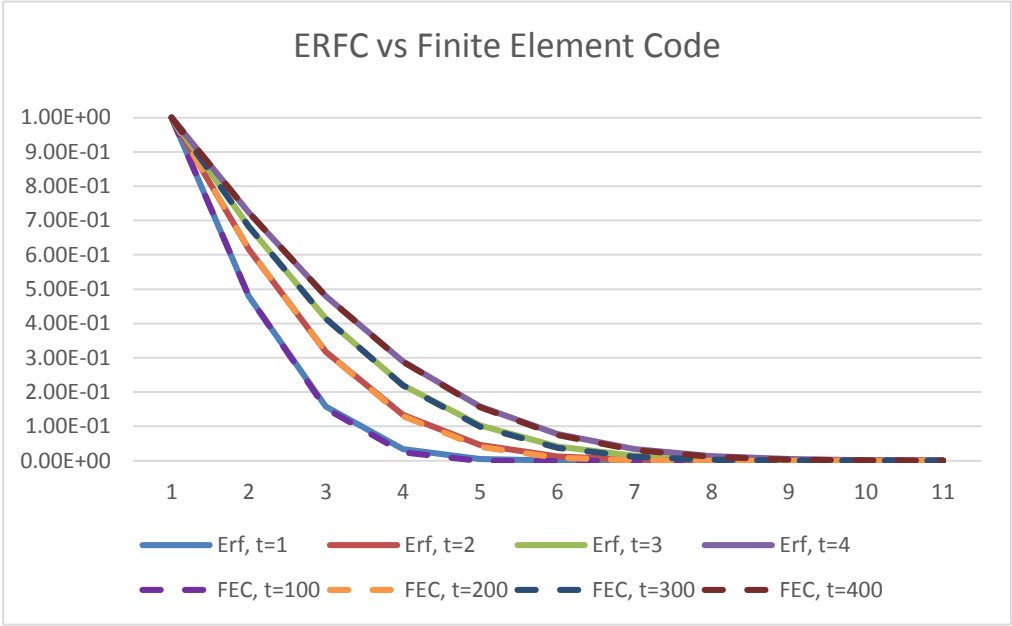

Figure 20: Finite Element Code vs Fortran ERFC outputs for the complementary error function

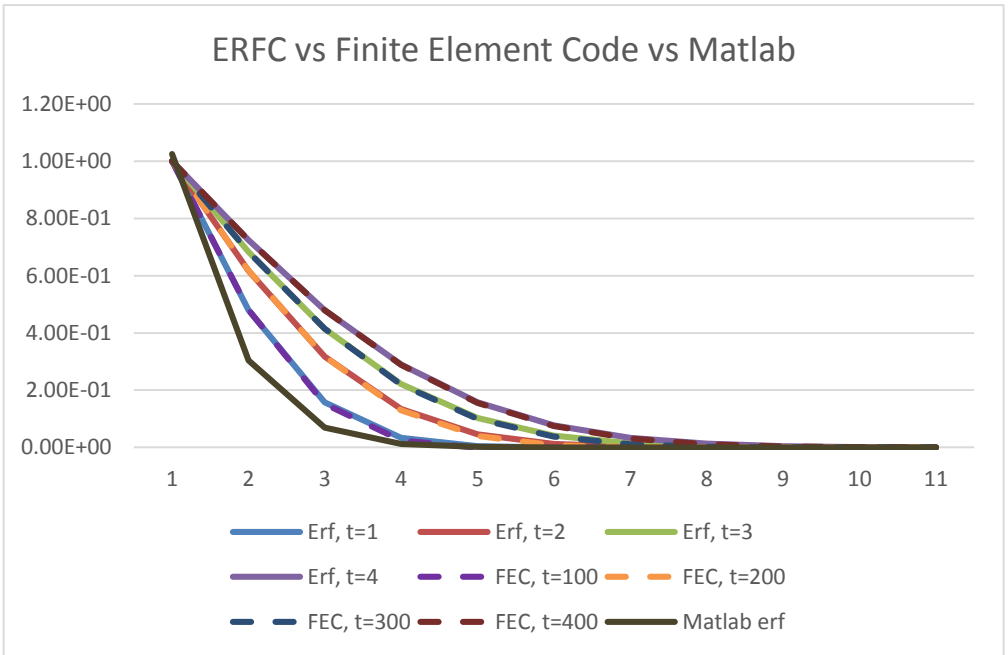

Figure 21: Finite Element Code vs Fortran ERFC vs Matlab outputs for the complementary error function

The Matlab code followed the template provided by Matlab for the partial differential equation function pdepe. The complete Matlab solution can be found in Appendix E. The results from the finite element erfc test were consistent with the Fortran erfc and Matlab code outputs. At this point, the finite element code was deemed accurate for modeling more complex problems involving the diffusion of moisture.

IV.3 Modeling Diffusion Using the Finite Element Code

Once it was established that the finite element code produced accurate results for a variety of input types, an input file was written to model the phenomenon under consideration – the effect of extended moisture exposure on asphalt pavement due to a rain event. Two material layers were modeled: an asphalt top layer and a soil base layer. The diffusivity of the asphalt layer was found in Chapter III to be 5.976E-5 cm^2/hr. For the soil base layer, a diffusivity of 6.84 cm^2/hr (1.9E-1 mm^2/sec) was used based on research reported by Lytton on movement in expansive clays (Lytton 1984). This diffusivity value is over one hundred thousand times the magnitude of the diffusivity measured for asphalt. Even the soils identified in the study as 'practically impervious', however, had diffusivities between 1.404 cm^2/hr and 2.88 cm^2/hr (3.9E-2 to 8.0E-2 mm^2/sec as recorded by Lytton), which are still twenty-five thousand times greater than the diffusivity found for asphalt found in this study.

A new two-dimensional mesh was generated with two hundred and thirty one nodes and four hundred elements divided into two different material layers, as shown in Figure 22. The top asphalt layer is modeled to be fifteen centimeters thick. An input file

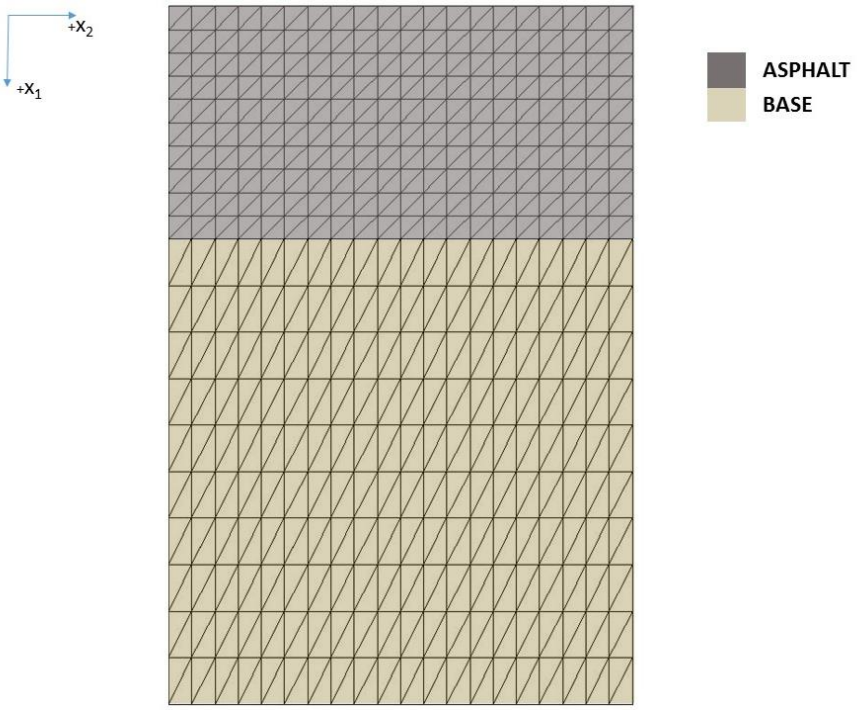

Figure 22: Two-dimensional finite element mesh

was built to model a transient process with sixty moisture boundary conditions – twenty across the top in the positive x_2 direction, ten down either side of the mesh in the positive x_1 direction, and twenty across the bottom, again in the positive x_2 direction. The moisture conditions on the bottom of the mesh as well as those running in the positive x_1 direction were assigned moisture values of zero. The moisture conditions on the top of the mesh were assigned moisture values of one. The input file was utilized to

run the finite element code and the resulting output was downloaded to Tecplot for visualization, as shown in Figure 23. Each time step represents two hours.

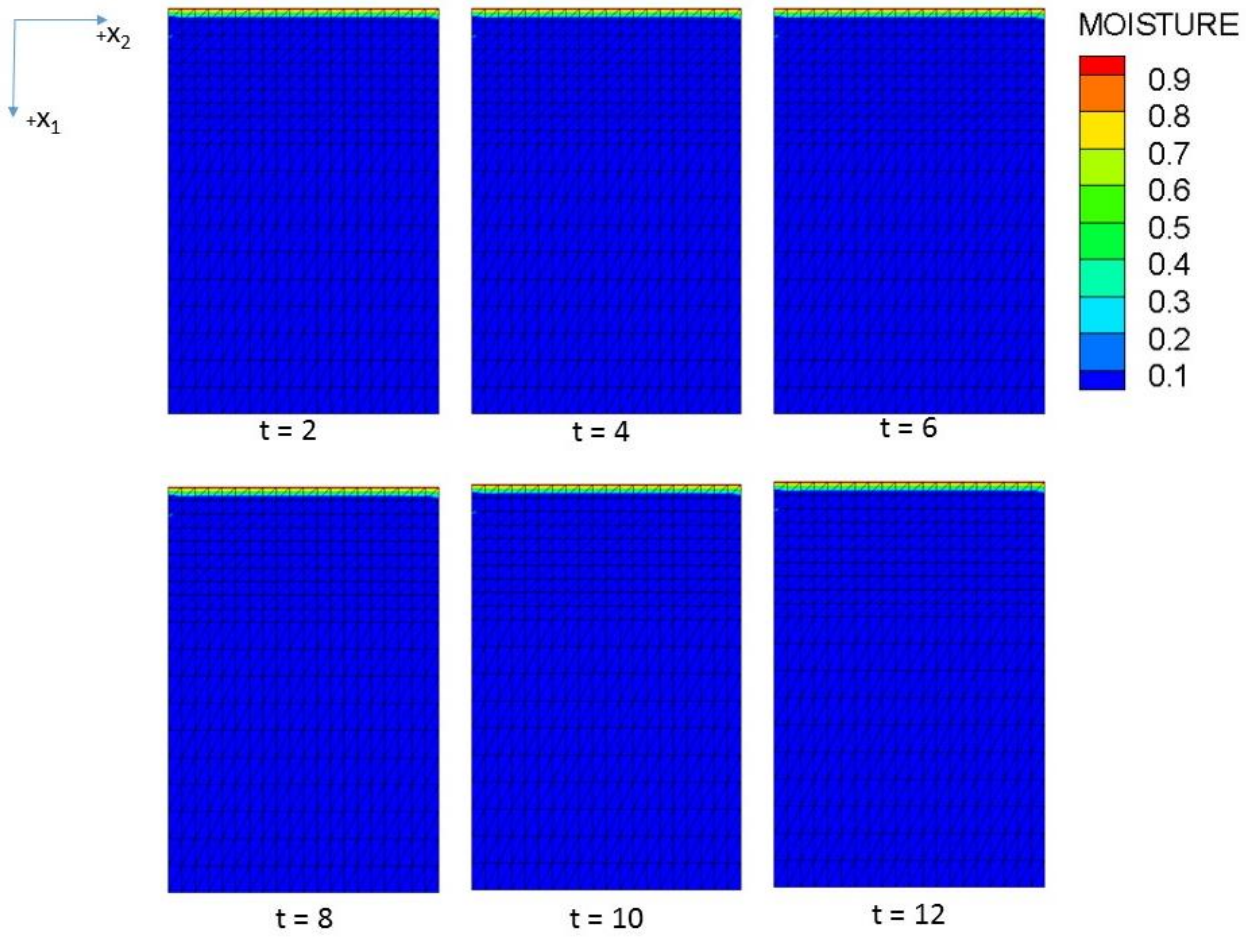

Figure 23: Tecplot modeling results of moisture movement in time

The results of the Tecplot visualization are consistent with the expected results for this model. Moisture is moving through the asphalt layer at an imperceptible pace. This suggests that a rain event producing moisture on the pavement for twelve hours or

less would not cause measureable damage to the asphalt layer or sub layers of a paved roadway. This is to be expected, as asphalt is designed to protect roadways from damage due to weathering.

How would the pavement and roadway behave, however, in the presence of a crack in the protective asphalt layer? To answer this question another mesh was created, this time with a crack included, but not fully splitting the asphalt layer (see Figure 24). The new mesh had four hundred and forty nine nodes and eight hundred elements divided in to two material models, the first ending with element four hundred, the second completing the mesh.

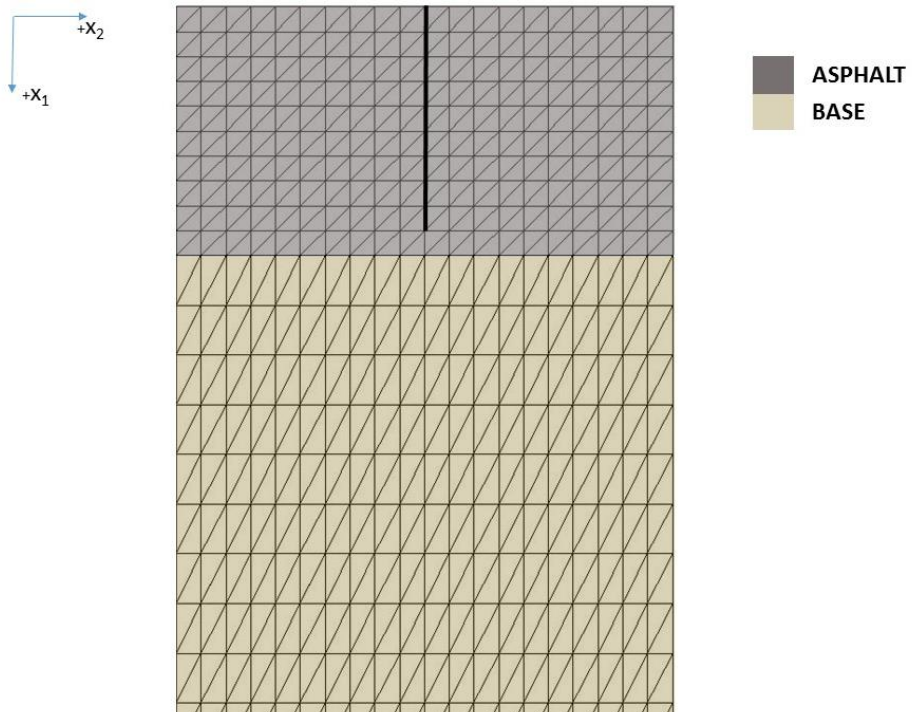

Figure 24: Finite element mesh with a partial crack in the asphalt concrete layer

The first material model is asphalt, assigned the experimental diffusivity found in Chapter III, and modeled to be fifteen centimeters thick. The second material property is a soil base layer, assigned a diffusivity of 6.84 cm^2/hr. An input file was built to model a transient process with fifty eight boundary conditions – twenty two across the top in the positive x_2 direction, fifteen down the center of the asphalt mesh layer direction beginning between points ten and eleven and traveling straight down in the positive x_1 direction, and twenty one across the bottom, again in the positive x_2 direction. The moisture conditions on the bottom of the mesh were assigned moisture values of zero. The moisture conditions on the top of the mesh as well as those going in the positive x_1 direction long the crack faces were assigned moisture values of one. The input file was run through the finite element code and the resulting output values were plotted using Tecplot for visualization (Figure 25).

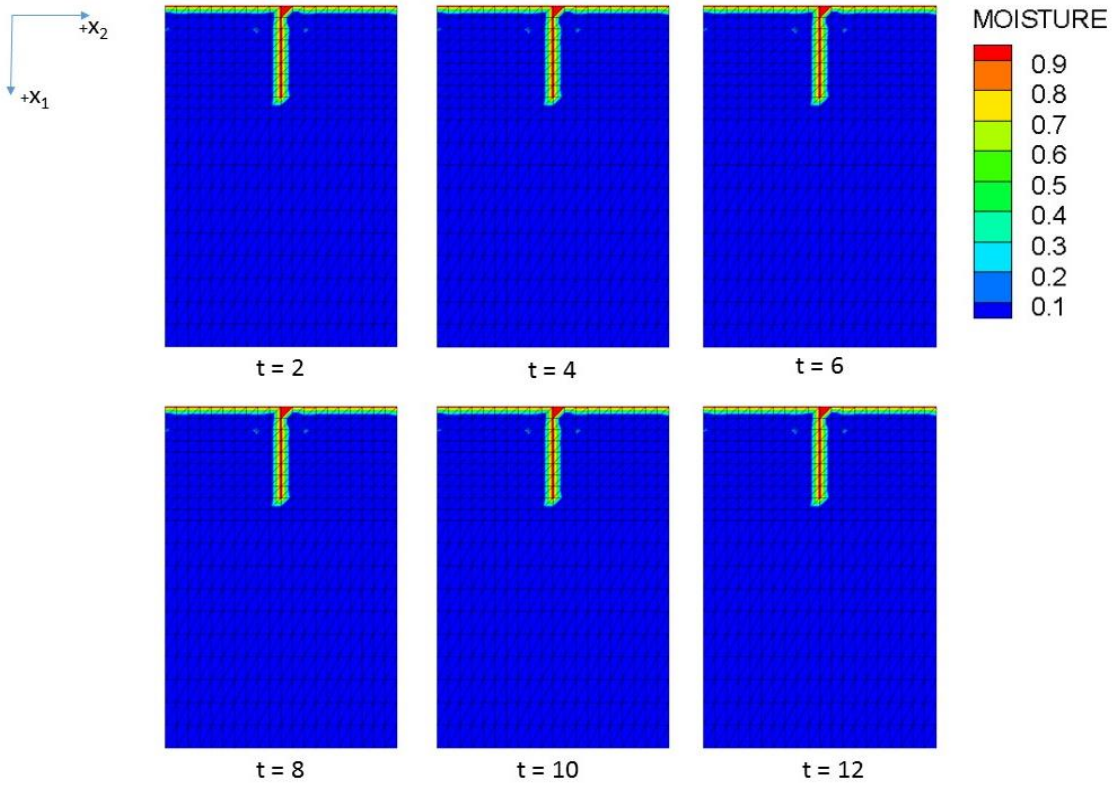

Figure 25: Predicted moisture distribution in time with a short crack

The predicted moisture distribution shows that the crack does not contribute significantly to moisture accumulation within the asphalt. Because the crack does not extend to the bottom of the asphalt concrete layer, insufficient moisture is predicted to reach the base layer. These results suggest that during a twelve-hour exposure with no freeze effect, a crack of this length would not contribute significantly to the degradation of the roadway.

Another finite element mesh was constructed to test the effect of the presence of a crack that extends completely through the asphalt concrete layer (see Figure 26). The

new mesh was constructed with four hundred and fifty two nodes and eight hundred elements divided into the two material models, arranged similarly to those in the first crack mesh, but with the crack extending into the base layer.

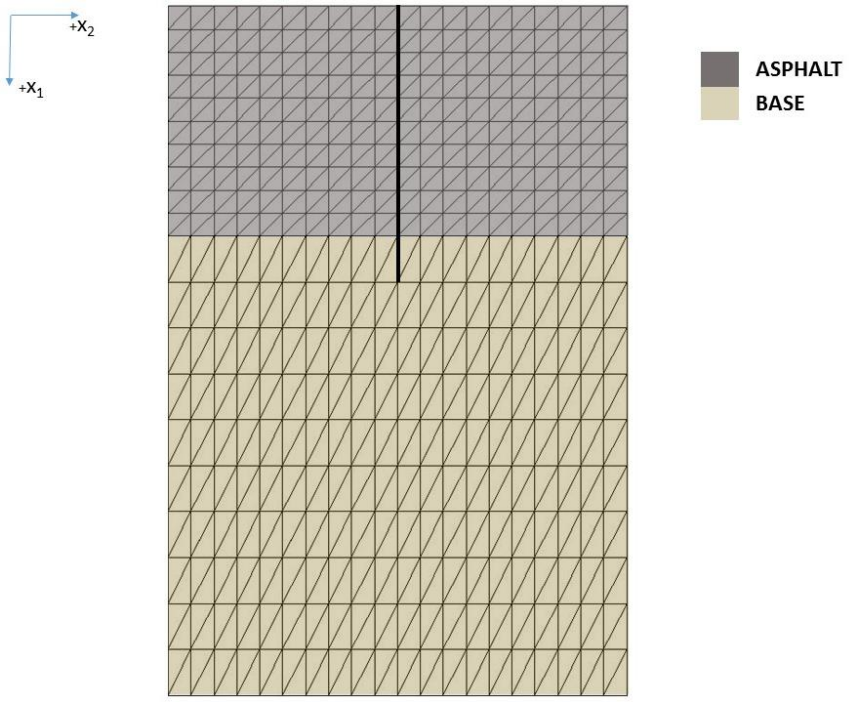

Figure 26: Finite element mesh with crack extending into the base layer

A new input file was built to model a transient process with sixty four boundary conditions to accommodate the longer crack length. The moisture conditions on the bottom of the mesh were assigned moisture values of zero. The moisture conditions on the top of the mesh as well as those going in the positive x_1 direction along the crack

faces were assigned moisture values of one. The input file was run in the finite element code and the resulting output values transferred to Tecplot for visualization (see Figure 27). The predicted moisture distribution for the long crack shows a dramatic difference

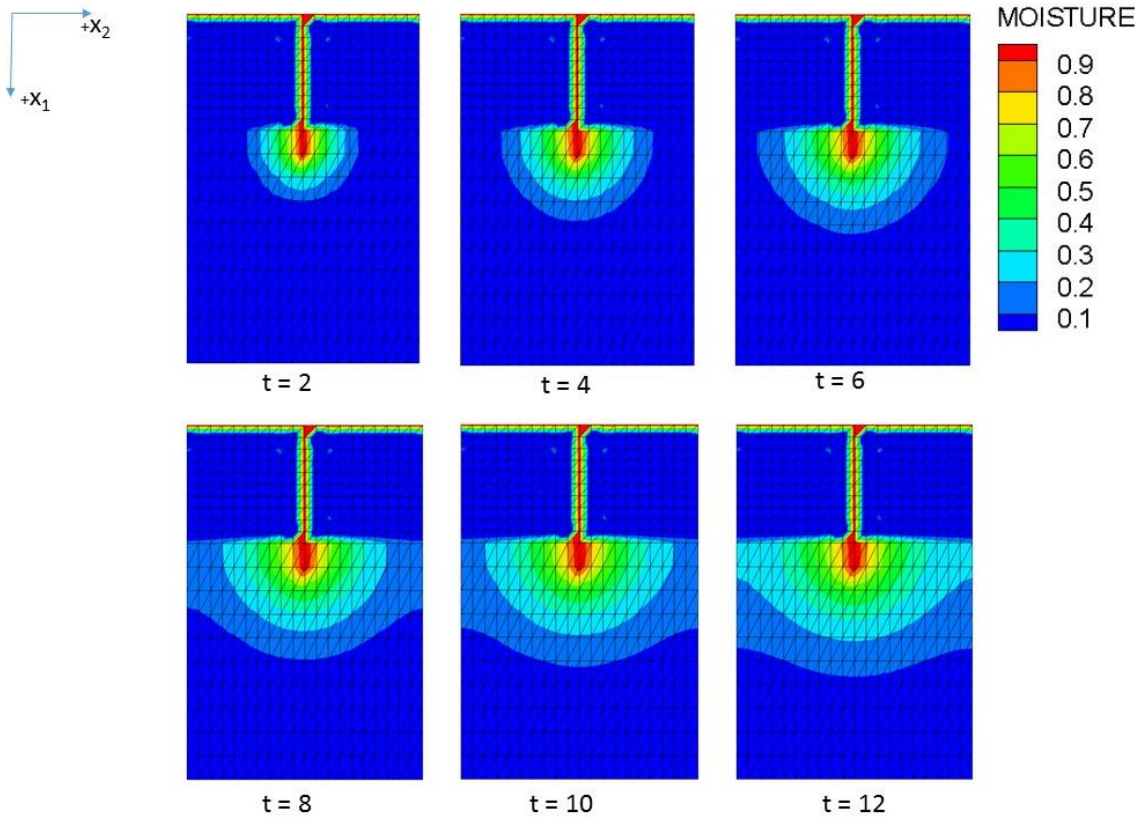

Figure 27: Predicted moisture distribution in time with a long crack

in moisture distribution from that predicted for a short crack. Moisture diffuses rapidly through the crack and into the base layer in sufficient quantities to cause swelling within

the base layer if the material is expansive. Since swelling of the base layer will likely induce bending in the already damaged asphalt concrete, it is concluded that when a crack extends completely through the asphalt layer, a rain event could potentially cause further cracking within the asphalt concrete in twelve hours or less.

IV.4 Conclusion

The Tecplot simulations indicate that undamaged asphalt is impermeable on a short time scale. The first simulation, shown in Figure 25, clearly showed that significant moisture does not accumulate within an undamaged asphalt layer or reach the soil base layer in twelve hours for typical values of diffusivity observed in asphalt concrete. The results of the second Tecplot simulation expanded on this, demonstrating that even with the presence of some damage in the form of a partial crack in the asphalt, significant moisture accumulation does not occur in the asphalt concrete, nor does moisture reach the soil base layer. However, the presence of a crack that completely splits the asphalt layer allows for significant moisture transport into the soil base layer. The dramatically higher soil diffusivity means that once moisture has travelled through the crack in the asphalt to reach the soil layer, moisture is rapidly transported deeper into the base material, creating the potential for greater damage due to moisture induced expansion of the subgrade.

In light of these results, future research should be conducted into how through-cracks form in asphalt concrete, and whether the presence of moisture in the base layer

contributes to the growth of subsequent cracks in the asphalt concrete layer. Additional research into the potential for sealing or healing of such cracks would also be well advised for the purpose of increasing durability of the roadway.

CHAPTER V

SUMMARY

Asphalt pavement is a multifaceted road construction material, making it complicated to model. With over 93% of America's roadways covered in asphalt, it is also one of the most important transportation materials in use, making it crucial that research be conducted into its behavior and degradation (NAPA 2015). Moisture contributes to the continued wearing of any pavement, and studying its mechanisms in asphalt can reveal some of the material's most fundamental properties. Being able to model the moisture gradient resulting from short-term liquid water exposure on the surface of the pavement will provide future researchers with necessary information to consider the effects of that moisture on such phenomena as base layer swelling, erosion, and freeze-thaw cycles.

This thesis has been concerned exclusively with the transport via diffusion of liquid water into and through the asphalt concrete layer of a roadway. Towards this end, Fick's Second Law was selected as an empirical model. Though it is known that moisture sorption in asphalt concrete does not always behave according to Fick's Second Law, it was determined that for the spatial and temporal scale at which the experiment was run the asphalt was satisfactorily statistically homogenous to apply Fick's Second Law. Accordingly, Fick's Second Law was inverted to determine the diffusivity of moisture in asphalt pavement, and tests were performed to determine this value experimentally within a typical asphalt concrete. The diffusion value was then applied within a finite element code written to model Fickian diffusion and three scenarios were modeled: an undamaged asphalt roadway, an asphalt roadway with a partial crack

through the asphalt concrete layer, and an asphalt roadway with a crack extending entirely through the asphalt concrete layer and into the base layer. The predicted results indicate that asphalt is nearly impermeable to water for short time durations. Only in the case where the crack extended entirely though the asphalt layer was significant water penetration predicted by the model, this occurring only in the base layer. These results suggest that asphalt roadways with partial cracks are not at risk for significant water damage over a short time period. However, there in the asphalt layer a crack that extends into the base layer, dramatic water damage to the roadway can occur in as a little as twelve hours.

Both the strength and weakness of this research is its simplicity. Fick's Second Law is easily and elegantly inverted to reveal diffusivity because of the absence of complicating coefficients related to suction or moisture retention. This study suggests that although asphalt is a heterogeneous material, Fick's Second Law can be accurately applied at certain length and time scales. In the future, continued research should be undertaken to better determine at what scale asphalt concrete can be modeled using Fick's Second Law and at what length and time scales the model loses accuracy. The experiment used in this research was also deceptively simple. The minimal design of the test samples – asphalt cores sealed in to PVC tubes – directly and succinctly created the necessary initial and boundary conditions for the experimental results to be used in conjunction with the empirical results. In an experiment of such low-tech simplicity used to measure such small changes, however, every aspect of the experimental process has the potential to cause inaccuracy. In the future, researchers should endeavor to find a

mass measuring scale on which the change in mass of the penetrating moisture can be experimentally measured with high precision. Weight measurement equipment is costly to purchase and delicate to maintain, but necessary for the accuracy of the model to be preserved. The weighing device used in this experiment could not weigh samples as massive or long as would have been ideal for this research. While the final specimen sizes were within the criteria outlined by Helms, et al, for statistical homogeneity, this limitation has the potential to mitigate the assumption of statistical homogeneity made when applying Fick's Second Law. Finally, the sealant employed should be studied more thoroughly and its viscoelastic and moisture related properties determined. The sealant is one of the only elements of the experimental setup that is not easily observed or controlled. There is inherent variation in its application that should be mitigated to the best of researchers' abilities.

The diffusivity found in this study, 5.976E-5 cm^2/hr, while within the range of acceptable values, is low when compared to similar studies in the field. Studies that have found values most similar to the one found here were conducted on FAM mixes, which have finer aggregates and lower void percentages. Because the specific components of the mix used in this research are not known, deeper comparison of the experimental results cannot be made. Additionally, the small sample size limits the conclusions that can be drawn. It is possible that the samples that were tested were denser or had fewer interconnected pores than an average sample, which would explain why they did not leak when others did. It is also possible that the dimensions of the asphalt cores tested (70 mm by 51 mm diameter) were in fact too small to ensure statistical homogeneity.

The best way to clarify these discrepancies would be to repeat the experiment with the same plant mix and many more samples of a larger size (additional length with an at least 76 mm diameter is recommended) to determine if the diffusivity value is consistent.

The findings of this research confirm that undamaged asphalt concrete is highly impervious to liquid water. The presence of just one crack, however, weakens the pavement to the point that it can rapidly degrade in the presence of moisture in as few as twelve hours. This encourages future research into the formation and correction of cracks in pavement. These findings also highlight the importance of a stable soil base layer that will not quickly erode or swell with moisture exposure. Additionally, while this study considered the effect of standing water, it would be interesting to investigate the effect that rushing water at the surface of the pavement would have on a permeating crack, as in a drainage structure or flood scenario. The addition of a surface flow model that incorporated momentum as well as mass flux at the surface of the pavement to the mass flux based diffusion model may produce interesting results.

REFERENCES

Amini, B. & Tehrani, S.S. 2014, "Simultaneous effects of salted water and water flow on asphalt concrete pavement deterioration under freeze–thaw cycles", *International Journal of Pavement Engineering,* vol. 15, no. 5, pp. 383-391.

Apeagyei, A.K., Grenfell, J.R. & Airey, G.D. 2015, "Application of Fickian and non-Fickian diffusion models to study moisture diffusion in asphalt mastics", *Materials and Structures,* vol. 48, no. 5, pp. 1461-1474.

Arambula, E., Caro, S. & Masad, E. 2009, "Experimental measurement and numerical simulation of water vapor diffusion through asphalt pavement materials", *Journal of Materials in Civil Engineering,* vol. 22, no. 6, pp. 588-598.

Arambula, E., Masad, E. & Martin, A.E. 2007, "Influence of air void distribution on the moisture susceptibility of asphalt mixes", *Journal of Materials in Civil Engineering,* vol. 19, no. 8, pp. 655-664.

Bulut, R. & Leong, E.C. 2008, "Indirect measurement of suction", *Geotechnical and Geological Engineering,* vol. 26, no. 6, pp. 633-644.

Cai, L. & Weitsman, Y. 1994, "Non-Fickian moisture diffusion in polymeric composites", *Journal of Composite Materials,* vol. 28, no. 2, pp. 130-154.

Caro, S., Masad, E., Bhasin, A. & Little, D.N. 2008, "Moisture susceptibility of asphalt mixtures, Part 2: characterisation and modelling", *International Journal of Pavement Engineering,* vol. 9, no. 2, pp. 99-114.

Chen, C. & Williams, R.C. 2014, "Water flow simulation and analysis in HMA microstructure", *Journal of Traffic and Transportation Engineering (English Edition),* vol. 1, no. 5, pp. 362-370.

Cheng, D., Little, D., Lytton, R. & Holste, J. 2003, "Moisture damage evaluation of asphalt mixtures by considering both moisture diffusion and repeated-load conditions", *Transportation research record: journal of the transportation research board,* vol. 1832, no. 6, pp. 42-49.

Cooley Jr, L., Brown, E. & Maghsoodloo, S. 2001, "Developing critical field permeability and pavement density values for coarse-graded superpave pavements", *Transportation Research Record: Journal of the Transportation Research Board,* vol. 1761, no. 6, pp. 41-49.

EPA 2014, *Porous Asphalt Pavement*. Available: http://water.epa.gov/polwaste/npdes/swbmp/Porous-Asphalt-Pavement.cfm [2015, August 26].

Ghauch, Z.G., Ozer, H. & Al-Qadi, I.L. 2015, "Micromechanical finite element modeling of moisture damage in bituminous composite materials", *Construction and Building Materials*, vol. 80, pp. 9-17.

Hansson, K., Lundin, L. & Šimůnek, J. 2005, "Part 3: Pavement: Subsurface Drainage and Reliability in Design and Performance: Modeling Water Flow Patterns in Flexible Pavements", *Transportation Research Record: Journal of the Transportation Research Board*, vol. 1936, no. 16, pp. 131-141.

Helms, K.L.E., Allen, D.H. & and Hurtado, L.D. 1999, "A Model for Predicting Grain Boundary Cracking in Polycrystalline Viscoplastic Materials Including Scale Effects", *International Journal of Fracture*, vol. 95, no. 1, pp. 175-194.

Hossain, M. 2014, "Modeling moisture-induced damage in asphalt concrete". Dissertation (PhD). The University of New Mexico.

Kassem, E., Masad, E., Bulut, R. & Lytton, R. 2006, "Measurements of moisture suction and diffusion coefficient in hot-mix asphalt and their relationships to moisture damage", *Transportation Research Record: Journal of the Transportation Research Board*, vol. 1970, no. pp. 45-54.

Kassem, E., Masad, E., Lytton, R. & Bulut, R. 2009, "Measurements of the moisture diffusion coefficient of asphalt mixtures and its relationship to mixture composition", *International Journal of Pavement Engineering*, vol. 10, no. 6, pp. 389-399.

Kim, Y., Little, D. & Lytton, R. 2004, "Effect of moisture damage on material properties and fatigue resistance of asphalt mixtures", *Transportation Research Record: Journal of the Transportation Research Board*, vol. 1891, no. 7, pp. 48-54.

Kringos, N., Scarpas, A. & Kasbergen, C. 2007, "Three Dimensional Elasto-Visco-Plastic Finite Element Model for Combined Physical-Mechanical Moisture Induced Damage in Asphaltic Mixes (With Discussion)", *Journal of the association of asphalt paving technologists*, vol. 76, pp. 495-524.

Kringos, N. & Scarpas, A. 2008a, "Physical and mechanical moisture susceptibility of asphaltic mixtures", *International Journal of Solids and Structures*, vol. 45, no. 9, pp. 2671-2685.

Kringos, N., Scarpas, A. & De Bondt, A. 2008b, "Determination of moisture susceptibility of mastic-stone bond strength and comparison to thermodynamical properties", *2008 Annual Meeting of the Association of Asphalt Paving Technologists, AAPT; Philadelphia, PA; 25 April 2008 through 30 April 2008*, pp. 435.

Kringos, N., Scarpas, T., Kasbergen, C. & Selvadurai, P. 2008c, "Modelling of combined physical–mechanical moisture-induced damage in asphaltic mixes, Part 1: governing processes and formulations", *International Journal of Pavement Engineering*, vol. 9, no. 2, pp. 115-128.

Kringos, N., Scarpas, A., Copeland, A. & Youtcheff, J. 2008d, "Modelling of combined physical–mechanical moisture-induced damage in asphaltic mixes Part 2: moisture susceptibility parameters", *International Journal of Pavement Engineering*, vol. 9, no. 2, pp. 129-151.

Legislative Budget Board 2011, *Texas Highway Funding: Legislative Primer*, 2nd edn, Legislative Budget Board Staff, Texas, USA.

Lehner, F. 1979, "On the validity of Fick's law for transient diffusion through a porous medium", *Chemical Engineering Science*, vol. 34, no. 6, pp. 821-825.

Lytton, R.L. 1994, "Prediction of movement in expansive clays", *Vertical and horizontal deformations of foundations and embankments* ASCE, pp. 1827.

NAPA, National Asphalt Pavement Association 2015, , *Engineering Overview*. Available: http://www.asphaltpavement.org/index.php?option=com_content&view=article&id=14&Itemid=33 [2015, August 26].

Raab, C., Partl, M. N., & El Halim, A. A. (2012). Experimental Investigations of Moisture Damage in Asphalt. *International Journal of Pavement Research and Technology*, *5*(3), 133.

Reddy, J.N. 1993, *An introduction to the finite element method*, McGraw-Hill New York.

SAS Institute Inc. 2013, *JMP Pro*, 11.0.0 edn, Cary, NC.

Sasaki, I., Moriyoshi, A., Hachiya, Y. & Nagaoka, N. 2006, "New Test Method for Moisture Permeation in Bituminous Mixtures", *Journal of the Japan Petroleum Institute*, vol. 49, no. 1, pp. 33-37.

Tarefder, R.A. & Yousefi, S.S. 2012, "Laboratory evaluation of moisture damage in asphalt", *Canadian Journal of Civil Engineering*, vol. 39, no. 1, pp. 104-115.

Vasconcelos, K.L., Bhasin, A., Little, D.N. & Lytton, R.L. 2010, "Experimental measurement of water diffusion through fine aggregate mixtures", *Journal of Materials in Civil Engineering*, vol. 23, no. 4, pp. 445-452.

Weitsman, Y. 1976, "Diffusion with time-varying diffusivity, with application to moisture-sorption in composites", *Journal of Composite Materials*, vol. 10, no. 3, pp. 193-204.

Yokoyama, T. & Nakashima, S. 2005, "Diffusivity anisotropy in a rhyolite and its relation to pore structure", *Engineering Geology*, vol. 80, no. 3, pp. 328-335.

APPENDIX A

DERIVATION OF THE COMPLEMENTARY ERROR FUNCTION

By applying the technique of integration by parts,

$$\int u(x)v'(x)dx = u(x)v(x) - \int v(x)u'(x)dx$$

$$u = erfc(z), \qquad dv = 1\,dz\,, \quad u'(z) = erfc(z)'dz, \quad v = z$$

where $erfc(z)' = \frac{-2e^{-z^2}}{\sqrt{\pi}}$ and z shares the limits of x

the expression becomes

$$\int_0^\infty erfc(z)\,dz = erfc(z) * z - \int_0^\infty z\left(\frac{-2e^{-z^2}}{\sqrt{\pi}}\right)dz \tag{I.47}$$

Apply substitution again to resolve $\int_0^\infty z\left(\frac{-2e^{-z^2}}{\sqrt{\pi}}\right)dz$. By u substitution,

$$u = -z^2\ ,\ du = -2z\,dz$$

Again, u shares the same limits as z. The expression becomes

$$\frac{1}{\sqrt{\pi}}\int_0^\infty e^u\,du$$

$$= \frac{1}{\sqrt{\pi}}(e^u + c)$$

$$= \frac{1}{\sqrt{\pi}}\left(e^{-z^2} + c\right)$$

$$= \frac{e^{-z^2}}{\sqrt{\pi}} + c \tag{I.48}$$

Plugging this back in the (I.47) results in

$$= \left[z * erfc(z) - \left(\frac{e^{-z^2}}{\sqrt{\pi}} + c\right)\right]_0^\infty \tag{I.49}$$

$$= \frac{1}{\sqrt{\pi}}$$

Bringing back the left side of equation (43), the completed expression is:

(I.50) $$\frac{M(t)}{Am_o(2\sqrt{Dt})} = \frac{1}{\sqrt{\pi}}$$

Solving for D,

$$\sqrt{D} = \frac{M(t)\sqrt{\pi}}{2Am_o\sqrt{t}}$$

(I.51) $$D = \frac{M(t)^2\pi}{4A^2m_o^2t}$$

APPENDIX B

VERIFYING THE INITIAL AND BOUNDARY CONDITIONS

(II. 1) $$D\frac{d^2m}{dx_1{}^2} = \frac{\partial m}{\partial t}$$

where $$m(x_1,t) = m_o erfc\left(\frac{x_1}{2\sqrt{Dt}}\right)$$

(II. 2) $$D\frac{d^2\left[m_o erfc\left(\frac{x_1}{2\sqrt{Dt}}\right)\right]}{dx_1{}^2} = \frac{\partial\left[m_o erfc\left(\frac{x_1}{2\sqrt{Dt}}\right)\right]}{\partial t}$$

The initial and boundary conditions are:

(II. 3) $m(x_1, t=0) = 0 \qquad 0 \le x_1 \le \infty$

(II. 4) $m(x_1 = 0, t) = m_o \qquad 0 \le t \le \infty$

(II. 5) $m(x_1 \to \infty, t) \to 0 \qquad 0 \le t \le \infty$

Verify that the initial condition is satisfied:

(II. 6) $$m(x_1,0) = m_o erfc\left(\frac{x_1}{2\sqrt{D(0)}}\right) = m_o erfc\left(\frac{x_1}{0}\right) = m_o erfc(\infty) = 0$$

Verify that the boundary conditions are satisfied:

(II. 7) $$m(0,t) = m_o erfc\left(\frac{0}{2\sqrt{Dt}}\right) = m_o erfc(0) = m_o$$

(II. 8) $$m(\infty,t) = m_o erfc\left(\frac{\infty}{2\sqrt{Dt}}\right) = m_o erfc(\infty) = 0$$

APPENDIX C

PROOF OF THE SOLUTION FOR DIFFUSIVITY

(III. 9) $$D\,\frac{d^2m}{dx_1{}^2} = \frac{\partial m}{\partial t}$$

where $$m(x_1,t) = m_o erfc\left(\frac{x_1}{2\sqrt{Dt}}\right)$$

and $$D = \frac{M(t)^2\pi}{4A^2m_o^2t}$$

(III. 10) $$D\,\frac{d^2\left[m_o erfc\left(\frac{x_1}{2\sqrt{Dt}}\right)\right]}{dx_1{}^2} = \frac{\partial\left[m_o erfc\left(\frac{x_1}{2\sqrt{Dt}}\right)\right]}{\partial t}$$

(III. 11) $$\left[\frac{M(t)^2\pi}{4A^2m_o^2t}\right]\frac{d^2\left[m_o erfc\left(\frac{x_1}{2\sqrt{\left[\frac{M(t)^2\pi}{4A^2m_o^2t}\right]t}}\right)\right]}{dx_1{}^2} = \frac{\partial\left[m_o erfc\left(\frac{x_1}{2\sqrt{\left[\frac{M(t)^2\pi}{4A^2m_o^2t}\right]t}}\right)\right]}{\partial t}$$

The t's in the denominators cancel:

(III. 12) $$\left[\frac{M(t)^2\pi}{4A^2m_o^2t}\right]\frac{d^2\left[m_o erfc\left(\frac{x_1}{2\sqrt{\left[\frac{M(t)^2\pi}{4A^2m_o^2}\right]}}\right)\right]}{dx_1{}^2} = \frac{\partial\left[m_o erfc\left(\frac{x_1}{2\sqrt{\left[\frac{M(t)^2\pi}{4A^2m_o^2}\right]}}\right)\right]}{\partial t}$$

The m_o in the numerator cancels

(III. 13) $$\left[\frac{M(t)^2\pi}{4A^2m_o^2t}\right]\frac{d^2\left[erfc\left(\frac{x_1}{2\sqrt{\left[\frac{M(t)^2\pi}{4A^2m_o^2}\right]}}\right)\right]}{dx_1{}^2} = \frac{\partial\left[erfc\left(\frac{x_1}{2\sqrt{\left[\frac{M(t)^2\pi}{4A^2m_o^2}\right]}}\right)\right]}{\partial t}$$

Solving the second order derivative on the left side of the expression first:

(III. 14) $$\frac{d^2\left[erfc\left(\frac{x_1}{2\sqrt{\left[\frac{M(t)^2\pi}{4A^2m_o^2}\right]}}\right)\right]}{{dx_1}^2}$$

Define $2\sqrt{\left[\frac{M(t)^2\pi}{4A^2m_o^2}\right]} = k = constant$

(III. 15) $$= \frac{d^2}{{dx_1}^2} erfc\left(\frac{x_1}{k}\right) = \frac{d}{dx_1}\left[-\frac{2e^{\left(\frac{-x_1}{k}\right)^2}}{\sqrt{\pi}} \cdot \left(\frac{1}{k}\right)\right]$$

where $\left(\frac{1}{k}\right)$ is the derivative of the expression inside the error function.

(III. 16) $$= \frac{-2}{k\sqrt{\pi}}\left[\frac{d}{dx_1} e^{\left(\frac{-x_1}{k}\right)^2}\right]$$

The derivative of $\left(\frac{-x_1}{k}\right)^2 = 2\left(\frac{-x_1}{k^2}\right)$, therefore

(III. 17) $$\frac{-2}{k\sqrt{\pi}}\left[\frac{d}{dx_1} e^{\left(\frac{-x_1}{k}\right)^2}\right] = \frac{-2}{k\sqrt{\pi}}\left[2\frac{-x_1}{k^2} e^{\left(\frac{-x_1}{k}\right)^2}\right]$$

By algebraic manipulation, $\frac{M(t)^2\pi}{4A^2m_o^2t} = \left(\frac{k}{2}\right)^2\frac{1}{t}$. Therefore, the left side of the (II.5) can be written as

$$\left(\frac{k}{2}\right)^2\frac{1}{t}\frac{-2}{k\sqrt{\pi}}\left[2\frac{-x_1}{k^2} e^{\left(\frac{-x_1}{k}\right)^2}\right] = \frac{x_1}{k\sqrt{\pi}} e^{\left(\frac{-x_1}{k}\right)^2}$$

$$= \frac{x_1}{2t\sqrt{\pi}\sqrt{\left[\frac{M(t)^2\pi}{4A^2m_o^2}\right]}} e^{\left(\frac{-x_1}{2\sqrt{\left[\frac{M(t)^2\pi}{4A^2m_o^2}\right]}}\right)^2}$$

Considering the right side of equation (III. 13),

$$\frac{\partial\left[erfc\left(\frac{x_1}{2\sqrt{\left[\frac{M(t)^2\pi}{4A^2m_o^2}\right]}}\right)\right]}{\partial t}$$

(III. 18)
$$= \frac{\partial}{\partial t}\left[erfc\left(\frac{x_1}{2\sqrt{\left[\frac{M(t)^2\pi}{4A^2m_o^2}\right]}}\right)\right]$$

In this context, x_1 is a constant, and $\frac{\pi}{4A^2m_o^2} = s = constant$

$$= \frac{\partial}{\partial t}\left[erfc\left(\frac{x_1}{2\sqrt{M(t)^2 \cdot s}}\right)\right]$$

$$= \left[-\frac{2e^{\left(\frac{-{x_1}^2}{4\cdot M(t)^2\cdot s\cdot m_o^2}\right)}}{\sqrt{\pi}}\right] \cdot \frac{d}{dt}\left[\frac{x_1}{2\sqrt{s}\,M(t)}\right]$$

(III. 19)
$$= \left[-\frac{2e^{\left(\frac{-{x_1}^2}{4\cdot M(t)^2\cdot s}\right)}}{\sqrt{\pi}}\right] \cdot \left[\frac{x_1}{2\sqrt{s}} \cdot \frac{d}{dt}\frac{1}{M(t)}\right]$$

When $D = \frac{M(t)^2\pi}{4A^2m_o^2t}$, $M(t) = \frac{Am_o\left(2\sqrt{Dt}\right)}{\sqrt{\pi}}$. Plugging that in,

$$= \left[-\frac{2e^{\left(\frac{-x_1}{2\sqrt{\left[\frac{M(t)^2\pi}{4A^2m_o^2}\right]}}\right)^2}}{\sqrt{\pi}}\right] \cdot \left[\frac{x_1}{2\sqrt{s}} \cdot \frac{d}{dt}\left(\frac{Am_o\left(2\sqrt{Dt}\right)}{\sqrt{\pi}}\right)^{-1}\right]$$

$$= \left[-\frac{2e^{\left(\frac{-x_1}{2\sqrt{\left[\frac{M(t)^2\pi}{4A^2m_o^2}\right]}} \right)^2}}{\sqrt{\pi}} \right] \cdot \left[\frac{x_1}{2\sqrt{s}} \cdot \left(\frac{Am_o 2\sqrt{D}}{\sqrt{\pi}} \right)^{-1} \frac{d}{dt}(t)^{-\frac{1}{2}} \right]$$

$$= \left[-\frac{2e^{\left(\frac{-x_1}{2\sqrt{\left[\frac{M(t)^2\pi}{4A^2m_o^2}\right]}} \right)^2}}{\sqrt{\pi}} \right] \cdot \left[\frac{x_1}{2\sqrt{s}} \cdot \left(\frac{Am_o 2\sqrt{D}}{\sqrt{\pi}} \right)^{-1} \left(-\frac{1}{2} t^{-\frac{3}{2}} \right) \right]$$

$$= -\frac{e^{\left(\frac{-x_1}{2\sqrt{\left[\frac{M(t)^2\pi}{4A^2m_o^2}\right]}} \right)^2}}{\sqrt{\pi}} \left[\frac{x_1}{\sqrt{s}} \cdot \left(\frac{Am_o 2\sqrt{D}}{\sqrt{\pi}} \right)^{-1} \left(-\frac{1}{2} t^{-\frac{3}{2}} \right) \right]$$

(III. 20)
$$= \frac{1}{2} \cdot \frac{e^{\left(\frac{-x_1}{2\sqrt{\left[\frac{M(t)^2\pi}{4A^2m_o^2}\right]}} \right)^2}}{\sqrt{\pi}} \left[\frac{x_1}{\sqrt{s}} \cdot \left(\frac{Am_o 2\sqrt{D}}{\sqrt{\pi}} \right)^{-1} \left(t^{-\frac{3}{2}} \right) \right]$$

Assemble both sides of the expression:

$$\frac{x_1}{2t\sqrt{\pi}\sqrt{\left[\frac{M(t)^2\pi}{4A^2}\right]}}e^{\left(\frac{-x_1}{2\sqrt{\left[\frac{M(t)^2\pi}{4A^2}\right]}}\right)^2}$$

$$= \frac{1}{2}\cdot\frac{e^{\left(\frac{-{x_1}^2}{4\left(\frac{Am_o\left(2\sqrt{Dt}\right)}{\sqrt{\pi}}\right)^2\frac{\pi}{4A^2}}\right)}}{\sqrt{\pi}}\left[\frac{x_1}{\sqrt{\frac{\pi}{4A^2}}}\cdot\left(\frac{Am_o 2\sqrt{D}}{\sqrt{\pi}}\right)^{-1}\left(t^{-\frac{3}{2}}\right)\right]$$

The $\frac{x_1}{2\sqrt{\pi}}e^{\left(\frac{-x_1}{2\sqrt{\left[\frac{M(t)^2\pi}{4A^2}\right]}}\right)^2}$ cancel in both expressions, leaving,

$$\frac{1}{t\sqrt{\left[\frac{M(t)^2\pi}{4A^2}\right]}} = \frac{1}{\sqrt{\frac{\pi}{4A^2}}}\cdot\left(\frac{Am_o 2\sqrt{D}}{\sqrt{\pi}}\right)^{-1}\left(t^{-\frac{3}{2}}\right)$$

Plug in $M(t) = \frac{Am_o\left(2\sqrt{Dt}\right)}{\sqrt{\pi}}$ on the left side

$$\frac{1}{t\sqrt{\frac{\left(\frac{Am_o\left(2\sqrt{Dt}\right)}{\sqrt{\pi}}\right)^2\pi}{4A^2}}} = \frac{1}{\sqrt{\frac{\pi}{4A^2}}}\cdot\left(\frac{Am_o 2\sqrt{D}}{\sqrt{\pi}}\right)^{-1}\left(t^{-\frac{3}{2}}\right)$$

$$\frac{1}{t\sqrt{\left(\frac{Am_o\left(2\sqrt{Dt}\right)}{\sqrt{\pi}}\right)^2}}\left[\frac{1}{\sqrt{\frac{\pi}{4A^2}}}\right] = \frac{1}{\sqrt{\frac{\pi}{4A^2}}}\cdot\left(\frac{Am_o 2\sqrt{D}}{\sqrt{\pi}}\right)^{-1}\left(t^{-\frac{3}{2}}\right)$$

$$\frac{1}{t\sqrt{\left(\frac{Am_o\left(2\sqrt{Dt}\right)}{\sqrt{\pi}}\right)^2}} = \left(\frac{Am_o 2\sqrt{D}}{\sqrt{\pi}}\right)^{-1}\left(t^{-\frac{3}{2}}\right)$$

$$\frac{1}{t\left(\frac{Am_o\left(2\sqrt{Dt}\right)}{\sqrt{\pi}}\right)} = \frac{1}{\left(\frac{Am_o 2\sqrt{D}}{\sqrt{\pi}}\right)\left(t^{\frac{3}{2}}\right)}$$

$$\frac{1}{\frac{Am_o\left(2\sqrt{Dt}\right)}{\sqrt{\pi}}} = \frac{1}{\frac{Am_o\left(2\sqrt{Dt}\right)}{\sqrt{\pi}}}$$

And the solution for *D* is proven.

APPENDIX D

MASS AND VOID PERCENTAGE PROPERTIES FOR THE ASPHALT SAMPLES USED TO FIND MOISTURE UPTAKE

Sample	Density	Voids %	Mass (g)	Mass PVC (g)	Assembled Mass (g)	Seran Mass (g)	Mass epoxy (g)
24114	2.27	7.30	295.90	117.973	422.04	422.520	8.168
24143	2.29	6.69	298.89	117.642	428.57	429.255	12.044
2711	2.22	9.44	294.06	115.479	417.81	418.308	8.273
27102	2.22	9.70	285.82	117.334	411.93	412.458	8.779
27103	2.23	9.22	289.13	117.433	416.38	416.848	9.812
27111	2.20	10.23	286.39	118.468	414.07	414.481	9.205
27113	2.22	9.33	288.62	118.175	416.77	417.305	9.982
27121	2.22	9.33	289.53	116.207	415.17	415.580	9.438
27122	2.22	9.54	286.46	116.839	415.14	415.818	11.839
27123	2.21	9.85	288.41	117.264	414.96	415.773	9.286

Table 4: Mass and percentage values for selected asphalt samples.

Note: Samples 24114, 27113, and 27122 were not included in the final calculations of diffusivity.

APPENDIX E

MATLAB CODE FOR THE ERROR FUNCTION SOLUTION OF THE PARTIAL DIFFERENTIAL EQUATION FOR FICK'S SECOND LAW

```
function fetest
% FUNCTION fetest
%
% m = defines symmetry of the problem:
%          slab = 0
%          cylindrical = 1
%          spherical = 2
% p = # of mesh points
% tstep = number of solution steps
%-------------------------------------------------------------

% INPUTS:
m = 0;
p = 10;
tstep = 10;

%-------------------------------------------------------------
x = linspace(0,p,p);
t = linspace(0,1,tstep);

% Run the PDE function:
% sol = pdepe(m, pdefun, icfun, bcfun, xmesh, tspan)
%   pdefun = handle to a function that defines the components of the PDE
%   icfun = handle to a function that defines the initial conditions
%   bcfun = handle to a function that defines the boundary conditions
%   xmesh = vector specifying the points at which a numercial solution is
%       requested for every value in tspan
%   tspan = vector specifying the points at which a solution is requested
%       for every value in xmesh

sol = pdepe(m,@fetestpde, @fetestic, @fetestbc, x, t);
% Extract the first solution component as u.
% ui = sol(j,:,i) approx the component i of the solution at time tspan(j)
%   and mesh points xmesh(:)
% want meshpoint p, time tspan
```

```
u = sol(tstep,:,1);

% Export the data to an Excel file:

xlswrite('matlaberfpde.xls',u);

% % Generate a solution profile (linear graph):
% figure
% plot(x,u(end,:))
% %axis([0 10 -1 2])
% title(sprintf('Solution at t = %d', tstep))
% xlabel('Distance x')
% ylabel(sprintf('u(x,%d)',tstep))
%---------------------------------------------------------------
%

end


function [ pl,ql,pr,qr ] = fetestbc( xl,ul,xr,ur,t )
% Defines boundary conditions for FUNCTION fetest
% 'l' and 'r' refer the left and right bounds
% p(x,t,u) + q(x,t,)f(x,t,u,du/dx) = 0
%   ul = approximate solution at the left boundary xl = a
%   ur = approximate solution at the right boundary xr = b
%   pl = column vector of p at xl
%   ql = column vector of q at xl
%   pr = column vector of p at xr
%   qr = column vector of q at xr

xl = 0;
xr = 10;
%
ul = 1;
ur = 0;

pl = 1;
ql = 1;
pr = 0;
qr = 1;

% pl = ul;
% ql = 0;
% pr = pi*exp(-t);
```

```
% qr = 1;
end


function u0 = fetestic( x )
% Defines the initial condition for FUNCTION fetest. This is given, not
% derived.

u0 = 0;


end


function [ c,f,s ] = fetestpde( x,t,u,DmDx )
% Defines the components of the PDE according to the equation:
% c(x,t,u,du/dx)du/dx = x^-m d/dx(c^mf(x,t,u,du/dx))+s(x,t,u,du/dx)

c = 1;
f = DmDx;
s = 0;

end
```

APPENDIX F

SAMPLE INPUT FILES FOR THE FINITE ELEMENT CODE

a. HINPUTEST1

```
1   6   4   0   1   4   0   0   1   0
1  0.0000000D+00  0.0000000D+00
2  1.0000000D+00  0.0000000D+00
3  0.0000000D+00  1.0000000D+00
4  1.0000000D+00  1.0000000D+00
5  0.0000000D+00  2.0000000D+00
6  1.0000000D+00  2.0000000D+00
1   1   3   4   1
2   2   1   4   1
3   3   5   4   1
4   4   6   5   1
1   2   5   6
      1.          1.          0.          0.
      1.          0.
      1.          1.0
```

b. HINPUTTEST5

```
 100   22   20    1    1    4    0    0    1    0
   0.1       0.5
 1  0.0000000D+00  0.0000000D+00
 2  1.0000000D+00  0.0000000D+00
 3  0.0000000D+00  1.0000000D+00
 4  1.0000000D+00  1.0000000D+00
 5  0.0000000D+00  2.0000000D+00
 6  1.0000000D+00  2.0000000D+00
 7  0.0000000D+00  3.0000000D+00
 8  1.0000000D+00  3.0000000D+00
 9  0.0000000D+00  4.0000000D+00
10  1.0000000D+00  4.0000000D+00
11  0.0000000D+00  5.0000000D+00
12  1.0000000D+00  5.0000000D+00
13  0.0000000D+00  6.0000000D+00
14  1.0000000D+00  6.0000000D+00
15  0.0000000D+00  7.0000000D+00
16  1.0000000D+00  7.0000000D+00
 17  0.0000000D+00  8.0000000D+00
18  1.0000000D+00  8.0000000D+00
19  0.0000000D+00  9.0000000D+00
20  1.0000000D+00  9.0000000D+00
21  0.0000000D+00  10.000000D+00
22  1.0000000D+00  10.000000D+00
 1   1   2   4   1
 2   1   4   3   1
 3   3   4   6   1
 4   3   6   5   1
 5   5   6   8   1
 6   5   8   7   1
 7   7   8  10   1
 8   7  10   9   1
 9   9  10  12   1
10   9  12  11   1
11  11  12  14   1
12  11  14  13   1
13  13  14  16   1
14  13  16  15   1
15  15  16  18   1
16  15  18  17   1
```

```
17   17   18   20    1
18   17   20   19    1
19   19   20   22    1
20   19   22   21    1
 1    2   21   22
        1.          1.          0.          0.
        1.          0.
        2400          1.5
```